Department of Energy
Carlsbad Field Office
P. O. Box 3090
Carlsbad, New Mexico 88221

NOV 2 1 2006

Mr. Juan Reyes
U.S. Environmental Protection Agency
1200 Pennsylvania Avenue, NW
Washington, D.C. 20460

Subject: Uncertainty Analysis for the Planned Change Request on Magnesium Oxide (MgO)
Emplacement

Dear Mr. Reyes:

This letter and its enclosures provide an uncertainty analysis that supports the U.S. Department of Energy's (DOE's) request for a reduction in the amount of magnesium oxide (MgO) emplaced at the Waste Isolation Pilot Plant (WIPP). The DOE currently emplaces 1.67 moles of MgO for every mole of organic carbon in cellulose, plastic, and rubber (CPR) materials that are emplaced in the WIPP. When the DOE requested that the MgO emplacement factor be reduced from 1.67 to 1.2 (letter Moody to Cotsworth, April 10, 2006), the EPA requested that the DOE address "the uncertainties related to MgO effectiveness, the size of the uncertainties, and the potential impact of the uncertainties on long-term performance" (letter Gitlin to Moody, April 28, 2006).

In response to the EPA's request, the DOE has analyzed the uncertainties associated with MgO. The enclosures to this letter document the results of the DOE's analyses. These enclosures are as follows:

- The *Overview of the MgO Uncertainty Analysis* is a brief, high-level summary of the key results from the uncertainty analysis and of the rationale for selecting an MgO emplacement factor of 1.2.
- The *Uncertainties Affecting MgO Effectiveness and Calculation of the MgO Effective Excess Factor* is the key technical report for the uncertainty analysis. It provides an integrated analysis for 15 types of uncertainty related to the effectiveness of MgO, and provides a quantitative assessment for the proposed MgO emplacement factor of 1.2.
- Four technical studies that evaluate specific aspects of repository response as they relate to the effectiveness of MgO. The technical studies evaluate: (i) the uncertainties related to carbonate precipitation, (ii) other uncertainties related to geochemistry, (iii) the amount of sulfate that could enter the repository from Castile brine and the amount of MgO that could be lost due to movement of that brine out of the repository, and (iv) the effectiveness of mixing processes in the repository.
- Two additional studies that evaluate the measurement uncertainty for CPR materials in the emplaced waste and the amount of reactive constituents in the bulk MgO supplied by Martin Marietta.

CBFO:AMO:RP:KJB:06-1415:UFC5486

These reports provide a comprehensive response to the EPA's request for an uncertainty analysis and to associated technical issues. If you have any questions regarding these reports, please contact Russell Patterson at (505) 234-7457.

Sincerely,

David C. Moody
Manager

cc: w/enclosures
D. Mercer, CBFO
G. Basabilvazo, CBFO
R. Lee, EPA
S. White, EPA
C. Byrum, EPA
T. Peake, EPA
S. Ghose, EPA
D. Kessell, SNL
N. Elkins, LANL
CBFO M & RC

OVERVIEW OF THE MgO UNCERTAINTY ANALYSIS

The U. S. Department of Energy (DOE) currently emplaces 1.67 moles of magnesium oxide (MgO) backfill for every mole of organic carbon in the cellulose, plastic, and rubber (CPR) materials that are emplaced in the Waste Isolation Pilot Plant (WIPP). The value of 1.67 represents a 67% excess over the amount of MgO that is required to react with the maximum amount of carbon dioxide that could be generated by microbial processes under conservative assumptions. The U. S. Environmental Protection Agency (EPA) has stated that this "relatively high excess amount" is required because "the extra MgO would overwhelm any perceived uncertainties that the chemical reactions would take place as expected" (Gitlin 2006). When the DOE requested that the MgO loading factor be lowered from 1.67 to 1.2, the EPA requested that the DOE address "the uncertainties related to MgO effectiveness, the size of the uncertainties, and the potential impact of the uncertainties on long-term performance" (Gitlin 2006).

The DOE's uncertainty analysis starts with a number of conservative assumptions: (i) microbes remain active through the lifetime of the repository, (ii) microbes will consume all of the organic carbon in the CPR materials that are emplaced in the repository, and (iii) other materials in the waste, such as lime and the corrosion products of iron-based materials, do not react with carbon dioxide (CO_2). The use of these assumptions maintains a conservative framework for determining the required amount of MgO in the repository.

The DOE evaluated 15 uncertainties related to MgO effectiveness, grouped into three categories:

1. Uncertainties in the quantities of CO_2 produced by microbial consumption of the organic carbon in the emplaced CPR materials
   a. Estimated amounts of CPR material in a room
   b. Effective yield of CO_2 per mole of emplaced organic carbon
   c. Role of methanogenesis

2. Uncertainties in the amount of MgO that is available to react with CO_2
   a. Fraction of reactive constituents in MgO
   b. Carbonation of MgO prior to emplacement
   c. Extent of reaction of MgO and/or brucite with CO_2
   d. Loss of MgO to brine outflow from the repository
   e. Likelihood of supersack rupture
   f. Amount of MgO in each room
   g. Efficiency of mixing processes
   h. Physical segregation of MgO from CO_2

3. Uncertainties in the moles of CO_2 sequestered per mole of MgO that is available to consume CO_2.
   a. Conversion of hydromagnesite to magnesite
   b. Consumption of CO2 by materials other than MgO
   c. Dissolution of CO_2 in WIPP brines
   d. Incorporation of CO_2 in biomass

Whenever possible, uncertainties were quantified and represented as random variables. The remaining uncertainties were reviewed qualitatively and are included via assumptions in the final estimation of MgO effectiveness. The results from the uncertainty analysis are dominated by Items 1b and 1c, the effective yield of CO_2 and the role of methanogenesis. These items are important because the yield of CO_2 per mole of organic carbon can be substantially less than previously assumed.

The uncertainty analysis for Items 1b and 1c has evaluated the yield of CO_2 per mole of organic carbon based on two microbial pathways: Pathway 1, when unlimited sulfate is always available from the waste and from natural sources, and Pathway 2, when sulfate is limited to that present in the emplaced waste. These two pathways represent the extremes in microbial gas generation because methanogenesis never occurs in Pathway 1 while it occurs to its maximum extent in Pathway 2. Further details on the pathways are provided in the report, *Uncertainties Affecting MgO Effectiveness and Calculation of the MgO Effective Excess Factor.*

For Pathway 1, enough sulfate enters the repository from the sulfate-bearing minerals and brine in the host rock to prevent methanogenesis; however, these minerals (anhydrite, gypsum, and polyhalite) also provide a natural source of calcium ions that can react with carbon dioxide, precipitating carbonate minerals. With precipitation of carbonate minerals, the uncertainty analysis demonstrates that the effective yield of CO_2 has a mean value of 0.72 moles of CO_2 per mole of organic carbon. For Pathway 2, methanogenesis consumes more than 94% of organic carbon in the waste and denitrification and sulfate reduction consume the remainder in the waste. Since methanogenesis produces 0.5 moles of CO_2 per mole of carbon and denitrification and sulfate reduction produce 1 mole of CO_2 per mole of carbon, the effective yield is given by 0.53 moles of CO_2 per mole of carbon in the waste. Thus, the effective yield of CO_2 lies within the narrow range of 0.53 to 0.72 moles of CO_2 per mole of organic carbon for the two pathways that represent the extremes of the microbial response.

The uncertainty analysis is based on an MgO loading factor of 1.2, consistent with the DOE's planned change request to the EPA. This loading factor implies a 20% excess of MgO if the effective yield is 1 mole of CO_2 per mole of organic carbon. However, this uncertainty analysis demonstrates that the excess amount of MgO is significantly greater than 20% because the expected yield of CO_2 is between 0.53 and 0.72. Conservatively taking the maximum value of the revised yield (0.72) into account, the full uncertainty analysis demonstrates that the mean or expected value of the effective loading factor is 1.6, or an excess MgO amount of 60%.

The uncertainty analysis also predicts a distribution for the effective loading factor, which defines the probability of having various excess amounts of MgO. The probability that the effective loading factor will be less than 1, the minimum amount of MgO required to sequester all CO_2, is of particular interest. The probability of an effective MgO loading factor less than 1 is calculated to be on the order of 10^{-19} for the distribution from this uncertainty analysis.

Given the conservative assumptions used in defining the 1.2 loading factor and the extremely small probability of a 1.2 loading factor not providing enough MgO to sequester all of the CO_2 generated, the uncertainty analysis provides confidence that an MgO loading factor of 1.2 defines a mass of MgO that will remain effective under all repository conditions.

Sandia National Laboratories
Waste Isolation Pilot Plant

Uncertainties Affecting MgO Effectiveness and Calculation
of the MgO Effective Excess Factor,
Revision 0

Author: Eric D. Vugrin (6711)

      Print   Signature   Date

Author: Martin B. Nemer (6711)

      Print   Signature   Date

Author: Steve Wagner (6711)

      Print   Signature   Date

Technical
Review: Mike Gross (WRES)

      Print   Signature   Date

QA
Review: Doug Edmiston (6710)

      Print   Signature   Date

Management
Review: Moo Y. Lee (6711)

      Print   Signature   Date

WIPP:1.4.1.2:PA:QA-L:543261

1.0 Executive Summary

The U. S. Environmental Protection Agency (EPA) currently requires the U. S. Department of Energy (DOE) to emplace 1.67 moles of magnesium oxide (MgO) in the Waste Isolation Pilot Plant (WIPP) for every mole of organic carbon in cellulose, plastic, and rubber (CPR) materials that is emplaced in the repository. The EPA has stated that they require this "relatively high excess amount" since "the extra MgO would overwhelm any perceived uncertainties that the chemical reactions would take place as expected" (Gitlin 2006). Consequently, when the DOE requested that the MgO excess factor be lowered from 1.67 to 1.2, the EPA requested that the DOE address "the uncertainties related to MgO effectiveness, the size of the uncertainties, and the potential impact of the uncertainties on long-term performance" (Gitlin 2006). To address this request, Sandia National Laboratories (SNL) has conducted an analysis of these uncertainties.

The analysis introduces the concept of the MgO "Effective Excess Factor" (EEF), a quantity that incorporates uncertainties into the current definition of the MgO excess factor. The uncertainties included in the EEF calculation are grouped into three categories:
1) uncertainties in the quantities of carbon dioxide (CO_2) produced by microbial consumption of the CPR;
2) uncertainties in the amount of MgO that is available to react with CO_2; and
3) uncertainties in the moles of CO_2 sequestered per mole of MgO that is available to consume CO_2. This uncertainty also includes materials other than MgO that could potentially sequester CO_2.

Whenever possible, these uncertainties were quantified and represented in the EEF calculation with random variables. The remaining uncertainties were qualitatively analyzed.

This analysis includes the conservative assumption that microbes will consume all of the organic carbon in the CPR materials that are emplaced in the repository. Though this analysis has not attempted to quantify the percentages of CPR materials that might be consumed or the probabilities associated with these percentages, inclusion of this uncertainty in calculation of the EEF has the potential to reduce the available organic carbon, thereby increasing the mean EEF.

Since the EEF considers the uncertainties affecting MgO effectiveness, it is necessary only for the EEF to be greater than 1.0 to maintain chemical conditions as assumed in WIPP Performance Assessment (PA). Using standard techniques from measurement theory, the quantified uncertainties of the individual components were propagated to calculate the mean and uncertainty for the EEF. If 1.2 moles of MgO are emplaced for every mole of organic carbon in emplaced CPR, the mean EEF is 1.60 and the standard deviation (uncertainty) is less than 0.0819.

Under the assumption that the EEF is lognormally distributed with mean equal to 1.60 and standard deviation equal to 0.0819, there is less than 10^{-19} probability that the EEF will be less than 1.01. Because the magnitude of this probability is so small and because many conservatisms have been incorporated into the calculation of the EEF, this analysis concludes that emplacing 1.2 moles of MgO for every mole of organic carbon in the emplaced CPR is more than sufficient to maintain chemical conditions as assumed in WIPP PA.

Table of Contents

List of Tables

List of Figures

2.0 Introduction

Magnesium oxide (MgO) is the only certified engineered barrier for the Waste Isolation Pilot Plant (WIPP), and it is emplaced in the repository along with the waste as a chemical control agent to mitigate the potential effects of significant microbial consumption of organic carbon in the cellulose, plastic, and rubber (CPR) materials in the post-closure repository environment (Appendix Barriers, DOE 2004a). The MgO backfill is emplaced to consume microbially generated carbon dioxide (CO_2), resulting in two primary consequences. First, consumption of the CO_2 buffers "the fugacity of CO_2 (f_{CO_2}) and pH [of brine] within ranges favorable from the standpoint of the speciation and solubilities of the actinides" (Appendix Barriers, DOE 2004a). An additional effect of the CO_2 consumption by MgO is that repository pressures are lower than would be expected in the absence of MgO. Previous performance assessments (PAs) have shown that repository pressures have a significant role in determining spallings releases, direct brine releases, and other aspects of repository performance.

Since 1996, the U. S. Department of Energy (DOE) has quantified the amount of MgO being emplaced in the repository in terms of an MgO "excess factor."[1] The DOE originally proposed placing one 4,000-lb MgO sack[2] (MgO super-sack) on top of each waste stack, as well as 25-lb MgO sacks (MgO mini-sacks) in between waste stacks and on the floor surrounding the waste, which resulted in an excess factor that was estimated to be 1.95 (DOE 1996). In June 2000, the DOE submitted a request to discontinue emplacement of MgO mini-sacks (DOE 2000), and in 2001, the U. S. Environmental Protection Agency (EPA) approved DOE's request to remove the MgO mini-sacks and lower the MgO excess factor to 1.67 (Marcinowski 2001).

On April 10, 2006, the DOE submitted a planned change request (PCR) to the EPA requesting approval to "emplace 1.2 moles of magnesium oxide (MgO) for every mole of consumable carbon contained in the Waste Isolation Pilot Plant (WIPP)" (Moody 2006). This amount of MgO represents a reduction from the 1.67 moles of MgO per mole of organic carbon that the EPA currently requires. In response to the DOE's request, the EPA indicated that "before EPA can evaluate DOE's request to lower the excess MgO emplaced to nearly the 'fully effective' range (1.00), DOE needs to address the uncertainties related to MgO effectiveness, the size of the uncertainties, and the potential impact of the uncertainties on long-term performance" (Gitlin 2006).

To address the EPA's request for additional information, Sandia National Laboratories (SNL) has conducted an analysis that reviews the uncertainties pertaining to the effectiveness of MgO and the calculation of the MgO excess factor. This report documents the uncertainty review and the results of this analysis. Section 3.0 reviews how the MgO excess factor is currently calculated and the assumptions and uncertainties related to this calculation. Additionally,

---

[1] DOE (1996, 2000), Marcinowski (2001), and other earlier documents related to MgO have discussed an MgO "safety factor" and "loading factor." Because Moody (2006) contends that this factor is not a safety factor in the truest engineering sense and the previous analyses have been concerned with having enough of an "excess" of MgO to overwhelm uncertainties, this analysis uses the term MgO "excess factor," and this term is intended to be synonymous with the term "safety factor."

[2] DOE originally proposed emplacing 4,000-lb supersacks. However, the DOE currently emplaces 4,200-lb supersacks (WTS 2005).

Section 3.0 introduces the concept of the MgO "Effective Excess Factor" (EEF), a quantity that incorporates the uncertainties affecting MgO effectiveness into the excess factor calculation. The three primary groups of uncertainties included in the EEF calculation are uncertainties affecting the quantity of carbon dioxide (CO_2) generated by microbial degradation of organic carbon, uncertainties affecting the quantity of MgO that is available to react with CO_2, and uncertainties affecting the number of moles of CO_2 that are consumed by a single mole of available MgO These categories are discussed in Sections 4.0, 5.0, and 6.0, respectively. The methods and techniques used to calculate the EEF and the resulting calculations are detailed in Section 7.0, and conclusions from this analysis are discussed in Section 8.0.

3.0 Calculation of the MgO Excess Factor

Currently, the MgO excess factor (EF) is defined as the product of two ratios: the ratio of the moles of emplaced MgO to the maximum number of moles of CO_2 that could be generated from microbial consumption of all of the organic carbon in the emplaced CPR materials and the ratio of the moles of CO_2 consumed per mole of emplaced MgO. This definition is represented by the following equation:

3-1
$$EF = \frac{M_{MgO}}{M_{CO_2}} \times \frac{1 \text{ mole of } CO_2 \text{ consumed}}{1 \text{ mole of MgO}}$$

The variable EF denotes the MgO excess factor, M_{MgO} represents the moles of emplaced MgO, and M_{CO_2} represents the maximum possible number of moles of CO_2 that could be generated by microbial consumption of all of the organic carbon in CPR materials. Presently, the EF is calculated for individual disposal rooms of the repository.

There are several inherent assumptions in the calculation of the excess factor.
1) It is conservatively assumed that all of the organic carbon in the emplaced CPR can and will be consumed by microbes.
2) It is conservatively assumed that this carbon will be consumed via denitrification and sulfate reduction, resulting in the maximum yield of 1 mole of CO_2 for every mole of consumed organic carbon.
3) It is assumed that every mole of emplaced MgO is available to react with CO_2.
4) It is assumed that every mole of MgO can consume 1 mole of CO_2 and that MgO sequestration will be the only mechanism for consumption of CO_2. The second ratio in Eq. 3-1 represents this assumption

Under these assumptions, emplacing an MgO excess factor of 1 is sufficient to maintain the PA assumption that MgO consumes all[3] CO_2 generated by microbial consumption of CPR materials.

---

[3] "Although MgO will consume essentially all CO_2, minute quantities (relative to the quantity that would be produced by microbial consumption of all CPR materials) will persist in the aqueous and gaseous phases" (Appendix Barriers, DOE 2004a). Because this quantity will be so small relative to the initial quantity, the adverb "essentially" is omitted in this document.

However, there are several uncertainties associated with each of these assumptions, and they can be grouped into four categories:

1) uncertainties in the quantities of CPR that will be consumed;
2) uncertainties in the quantities of CO_2 produced by microbial consumption of the organic carbon in CPR materials;
3) uncertainties in the amount MgO that is available to consume CO_2; and
4) uncertainties in the moles of CO_2 sequestered by each mole of available MgO. This uncertainty also includes materials other than MgO that could potentially sequester CO_2.

The purpose of this analysis is to determine the impact of these uncertainties on the excess factor calculation. In order to do so, this analysis introduces the concept of the MgO "Effective Excess Factor." This term incorporates uncertainties 2) – 4) listed above and is defined as follows:

3-2
$$\text{EEF} = \frac{\text{available moles of MgO}}{\text{moles of } CO_2 \text{ produced}} \times \frac{\text{moles of } CO_2 \text{ consumed}}{1 \text{ mole of MgO}} = \frac{m \times M_{MgO}}{g \times M_C} \times r.$$

The term M_C denotes the total moles of organic carbon in the emplaced CPR mass, and M_{MgO} is the total moles of MgO (defined previously in Eq. 3-1). The random variables g, m, and r represent the uncertainty in the quantities of CO_2 produced per mole of consumed organic carbon, the uncertainty in the amount of MgO available for CO_2 consumption, and the uncertainty in the moles of CO_2 sequestered per mole of emplaced MgO, respectively. (These variables are further defined and discussed in the Sections 4.0-6.0). Because these uncertainties are included in the EEF calculation, an EEF greater than 1.0 would indicate that sufficient MgO is being emplaced to ensure that chemical reactions will "take place as expected" and that PA assumptions related to the consumption of CO_2 are maintained.

It should be noted that the calculation of the MgO EEF still includes the conservative assumption that all of the organic carbon in the CPR materials can and will be consumed by microbes. In keeping with the EPA's direction that "DOE needs to address the uncertainties related to MgO effectiveness, the size of the uncertainties, and the potential impact of the uncertainties on long-term performance" (Gitlin 2006), the uncertainties associated with this assumption are qualitatively discussed in Appendix A.

4.0 Quantities of CO_2 Produced by Microbial Respiration

The amount of CO_2 that could be produced if all of the carbon in the emplaced CPR is consumed is the product of the moles of carbon in the emplaced CPR materials and the number of moles of CO_2 produced per mole of consumed carbon (i.e., the effective CO_2 yield). This calculation is expressed in the following equation:

4-1
$$\text{moles of } CO_2 = y_{yield} \times M_C.$$

The term M_C represents the moles of carbon in CPR, and y_{yield} represents the effective CO_2 yield (in moles of CO_2 per mole of consumed carbon).

Two categories of uncertainties affect the quantities of CO_2 that can be produced via microbial respiration. First, there is uncertainty in the quantity of emplaced CPR. The DOE estimates the quantity of CPR materials in each waste container that is shipped to the WIPP, and there is

uncertainty associated with these estimates. Secondly, there is uncertainty in which microbial respiration pathway is utilized for consumption of CPR materials. Because different pathways result in different amounts of CO_2 produced per mole of consumed carbon, this uncertainty has the potential to impact the amount of CO_2 that could be produced. Hence, the denominator in Eq. 3-2 can be rewritten in the following form:

4-2 $$\text{moles of CO}_2 \text{ produced} = y_{yield} \times y_{CPR} \times M_C$$

where y_{CPR} and y_{yield} are random variables that represent the uncertainty in the moles of carbon emplaced relative to the amount reported by DOE and the uncertainty in the moles of CO_2 yielded per mole of consumed carbon when all of the CPR is consumed, respectively.

4.1 *CPR Estimates*

Kirchner and Vugrin (2006) quantified the uncertainties in DOE's CPR estimates. In this analysis, an examination of the potential errors in the CPR mass estimates made using Real Time Radiography (RTR) showed that the effect of errors in these measurements is unlikely to cause the uncertainty in the total mass of CPR for a room to be of any practical significance. The analysis was based on differences between the Visual Examination (VE) and RTR estimates of mass paired by containers from various TRU waste sites. In this analysis the VE estimates were assumed to be the more accurate value and were treated as the true values. Monte Carlo methods were used to simulate potential errors in the RTR measurements and to construct a distribution representing the uncertainty in the total CPR quantity in a room. These results confirm that the relative uncertainty (defined as the standard deviation divided by the mean in Kirchner and Vugrin (2006)) on the total mass of CPR in a room would be less that 0.3%. Because no significant bias was observed in the RTR measurements, it is appropriate to assume that the total of the CPR estimates is the best estimate of the true value of the total mass of CPR.

In addition to quantifying the error in CPR measurements from RTR, Kirchner and Vugrin (2006) also bounded the relative uncertainty on the total mass of CPR from both RTR and VE in a room. For this assessment, the RTR and VE estimates are both assumed to be unbiased estimates of the true CPR mass, and Kirchner and Vugrin (2006) conclude that the relative uncertainty on the total mass of CPR from both RTR and VE in a room is bounded above by the 0.3%. This uncertainty is so small that its impact on calculating the MgO excess factor is negligible.

The number of containers in a disposal room has the potential to affect the relative uncertainty of the total mass of CPR in a room. Kirchner and Vugrin (2006) assume that each disposal room contains 11,000 55-gallon drums, but actual disposal rooms may contain more or less than this number. Vugrin (2006) indicates that the number of supersacks per room in Panel 2 and in filled rooms in Panel 3 (rooms 4, 5, 6, 7) ranges between 363 and 540 supersacks[4]. To estimate the number of containers per room, one can assume that each supersack corresponds to one waste stack comprised of three 7-packs of 55-gallon drums. Thus, the number of containers in each room ranges between 7,623 and 11,340 containers ($363 \times 21 = 7,623$ and $540 \times 21 = 11,340$).

---

[4] Because some rooms in Panel 1 were not completely filled, only the rooms in Panels 2 and 3 are used to determine the expected number of containers per room.

Using the lower bound of 7,623 containers per room and the second equation from Section 4.4.2 of Kirchner and Vugrin (2006), the relative uncertainty on the total mass of CPR in a room is calculated to be 0.00246. Hence, the relative uncertainty on the total mass of CPR in a room is still less than 0.3% when the lower bound of containers per room is used.

Hailey (1994) conducted a comparison of individual RTR and VE estimates for a variety of waste characteristics, including CPR content. The analysis included CPR estimates for 32 drums from a single waste shipping site (Idaho National Laboratory). The analysis only compared estimates for individual drums and did not attempt to quantify the variability on the entire population of drums examined. Hailey (1994) noted that there were large differences between the RTR and VE CPR estimates for some containers, but Hailey (1994) did not discuss whether or not there was a bias in the estimation techniques.

Some of the individual containers included in the Kirchner and Vugrin (2006) analysis had large differences between the RTR and VE estimates of CPR, but Kirchner and Vugrin (2006) concluded that there was no bias in the estimates. Thus, due to "the large number of containers whose CPR masses are added to calculate the total CPR content in a room, random errors are expected, overall, to cancel out since overestimates of mass in some containers are compensated by underestimates of mass in other containers" (Kirchner and Vugrin 2006). This analysis will use the results from Kirchner and Vugrin (2006) rather than Hailey (1994) for the following reasons:
1) The number of drums included in the Kirchner and Vugrin (2006) analysis is more than 6 times the number of drums that Hailey (1994) compared.
2) Kirchner and Vugrin (2006) included drums from 3 waste shipping sites whereas Hailey (1994) analyzed drums from a single site.
3) The appropriate scale to examine uncertainties in CPR quantities is the room scale since the MgO EF is tracked on a per room basis. Hailey (1994) only considers estimates on a per drum basis.

Hence, the random variable y_{CPR} that represents the moles of carbon emplaced relative to the amount reported by DOE is assigned a mean value, μ_{CPR}, of 1.0, i.e. the mean CPR quantity in a room is equal to the sum of the CPR quantities in the individual containers that DOE reports. The standard deviation of y_{CPR}, σ_{CPR}, is conservatively set equal to 0.003, the upper bound on the relative uncertainty in the amount of CPR in a single room.

4.2 Microbial Respiration Pathways

Wang and Brush (1996) identify three potentially significant microbial respiration pathways in the repository: denitrification (Eq. 4-3), sulfate (SO_4^{2-}) reduction (Eq. 4-4), and methanogenesis (Eq. 4-5). These reaction pathways are described by the following equations:

4-3
$$C_6H_{10}O_5 + 4.8H^+ + 4.8NO_3^- \rightarrow 7.4H_2O + 6CO_2 + 2.4N_2;$$

4-4
$$C_6H_{10}O_5 + 6H^+ + 3SO_4^{2-} \rightarrow 5H_2O + 6CO_2 + 3H_2S;$$

4-5
$$C_6H_{10}O_5 + H_2O \rightarrow 3CH_4 + 3CO_2.$$
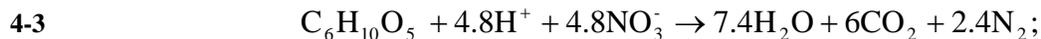
These reactions are assumed to proceed sequentially as each electron acceptor (NO_3^-, SO_4^{2-}) is consumed. The yield is 1 mole of CO_2 per mole of organic carbon consumed from denitrification and SO_4^{2-} reduction, and 0.5 moles of CO_2 per mole of organic carbon consumed from methanogenesis.

For the 2004 Compliance Recertification Application (CRA-2004), Snider (2003a) estimated that if all of the CPR materials in the inventory were consumed sequentially by these pathways, (1) 4.72 mole % of the organic carbon in CPR materials will be consumed by denitrification, 0.82 mole % by SO_4^{2-} reduction, and 94.46 mole % by methanogenesis; and (2) if all of the organic carbon is consumed, the overall CO_2 yield will be 0.53 moles of CO_2 per mole of organic carbon consumed. The calculations by Snider (2003a) only considered the emplaced waste as a possible source of sulfate. However, for the 2004 Compliance Recertification Application (CRA-2004) Performance Assessment Baseline Calculation (PABC), methanogenesis was not included because of the EPA's concern that there is enough sulfate available in the surrounding disturbed rock zone (DRZ) to maintain sulfate reduction indefinitely. The EPA directed that for the CRA-2004 PABC, only denitrification and sulfate reduction be considered as viable microbial respiration pathways for CO_2 generation (Cotsworth 2005). Consequently, when the updated inventory for the CRA-2004 PABC is considered, 4.89 mole % of the organic carbon in CPR materials will be consumed by denitrification and 95.11 mole % by SO_4^{2-} reduction when all of the organic carbon is consumed. Sulfate reduction that uses only sulfate in the waste materials will consume 0.84 mole % of the organic carbon. (Appendix B details the calculation of these percentages.) Exclusion of methanogenesis resulted in a yield of 1.0 moles of CO_2 per mole of organic carbon consumed for the CRA-2004 PABC.

Clearly, uncertainty in microbial respiration pathways affects the uncertainty in the total amount of CO_2 that could be generated, and the following sections detail how this uncertainty is quantified for the EEF calculation. Section 4.2.1 discusses the different sources of sulfate in and near the repository and that some minerals in the DRZ contain significant sources of calcium along with the sulfate. Section 4.2.1.1 details the mechanism for transporting sulfate and calcium from the DRZ into the waste areas of the repository and how the precipitation of $CaCO_3$-bearing minerals can impact effective CO_2 yields when sulfate reduction occurs. The quantity of sulfate that could enter the repository from Salado and Castile brines is discussed in Section 4.2.1.2, and uncertainties related to methanogenesis are discussed in Section 4.2.2. Finally, Section 4.2.3 incorporates all of the uncertainties related to the microbial respiration pathways into a single calculation to determine an effective CO_2 yield.

4.2.1 Sulfate Reduction

There are three possible sources of sulfate for microbial consumption of carbon via sulfate reduction (Kanney et al. 2004):
1) emplaced waste materials;
2) brine stored in the Salado formation and the Castile formation that underlies the Salado (Deal et al. 1995, Popielak et al. 1983); and
3) sulfate-bearing minerals such as anhydrite, gypsum and polyhalite in the Salado rock surrounding the disposal rooms (DOE 1983a,b).

A distinguishing characteristic between the brine sulfate source and the sulfate in the sulfate-bearing minerals is the quantity of calcium present along with the sulfate, and as will be shown in Section 4.2.1.1, the source of sulfate can have a significant impact on the effective CO_2 yield.

Two analyses were conducted to assess the impact of the sulfate sources on the effective CO_2 yield. Brush et al. (2006) assessed the impact of calcium on the effective CO_2 yield when organic carbon is consumed via sulfate reduction with sulfate from the surrounding minerals, and the results of this analysis are summarized in Section 4.2.1.1. Clayton and Nemer (2006) conducted an analysis that calculated quantities of Castile sulfate that could enter a single waste panel in the repository, and the results of that analysis are discussed in Section 4.2.1.2. Section 4.2.1.2 also explains this analysis conservatively assumes that the Salado brines are not a significant source of sulfate.

4.2.1.1 Precipitation of Carbonate Minerals

It has been hypothesized that sulfate could be transported into the disposal rooms by diffusive transport from the surrounding minerals. Brush et al. (2006) describes the transport process in the following manner:

> *"Diffusive transport of SO_4^{2-} from the Salado to the disposal rooms – if it occurs to a significant extent – would occur because microbial SO_4^{2-} reduction would consume the SO_4^{2-} in the waste and in brines in contact with the waste via* [Eq. 4-4], *thereby creating a concentration gradient from the DRZ to the waste. If SO_4^{2-} diffuses from the DRZ through saturated voids to the waste, the dissolved SO_4^{2-} concentrations in the DRZ would decrease. However, this decrease would result in dissolution of SO_4^{2-}-bearing minerals such as anhydrite, gypsum $(CaSO_4 \cdot 2H_2O)$, and polyhalite $(K_2MgCa_2(SO_4)_4 \cdot 2H_2O)$, present in both the marker beds and the nearly pure halite (NaCl) in the Salado."*

Brush et al. (2006) further explain that the dissolution of sulfate bearing minerals "would yield abundant Ca^{2+} if microbes use naturally occurring SO_4^{2-} to a significant extent after consuming all SO_4^{2-} in the waste." The presence of large quantities of Ca^{2+} in the waste areas is significant because the "Ca^{2+} released … would consume CO_2 by precipitating calcite ($CaCO_3$), metastable polymorphs of calcite, hydrated $CaCO_3$, or minerals such as pirssonite ($Na_2Ca(CO_3)_2 2H_2O$)" (Brush et al. 2006), and consequently, the calcium could impact the CO_2 yield. Consumption of CO_2 by precipitation of $CaCO_3$–bearing minerals reduces the amount of MgO that must be emplaced for CO_2 sequestration, hence, impacting the EEF calculation.

Brush et al. (2006) conducted an analysis in which the primary objective was to calculate the effective CO_2 yield when precipitation of $CaCO_3$–bearing minerals is considered as a potential mechanism for consumption of CO_2. Brush et al. (2006) define the effective CO_2 yield to be the number of moles of CO_2 produced per mole of consumed carbon, after allowing for consumption of CO_2 by precipitation of $CaCO_3$ or $CaCO_3$-bearing minerals. To do this, Brush et al. (2006) used the reaction path code EQ6 (Wolery and Daveler 1992) to simulate the precipitation of carbonate minerals caused by the reaction of microbial CO_2 with Ca^{2+}during sulfate reduction. A series of simulations were run to assess the sensitivity of effective CO_2 yields (and other

outputs) to the following factors: "(1) the initial brine composition and the brine volume, (2) whether carbonation of brucite produces magnesite or hydromagnesite, (3) the effects of organic ligands, and (4) the effects of precipitation of $CaCO_3$(am) instead of calcite." For each of the simulations, the following assumptions were made:

1) All of the organic carbon in the emplaced CPR materials is consumed by microbial respiration.
2) 4.89 mole % of the organic carbon is consumed via denitrification.
3) 0.84 mole % of the organic carbon is consumed via sulfate reduction with sulfate in waste materials.
4) The remaining 94.27 mole % of the organic carbon is consumed via sulfate reduction with sulfate from the surrounding minerals.

Brush et al. (2006) report four effective yields for each simulation:

1) The effective CO_2 yield during the denitrification step. This yield is always 1 mole of CO_2 per mole of consumed carbon.
2) The effective CO_2 yield when sulfate reduction proceeds with sulfate from the waste materials. This yield is always 1 mole of CO_2 per mole of consumed carbon.
3) The effective CO_2 yield when sulfate reduction proceeds with sulfate from DRZ minerals. This yield is equal to the fraction of the CO_2 that is consumed by either magnesite or hydromagnesite, depending on the simulation. This yield ranged from 0.54 to 0.60 moles of CO_2 per mole of consumed organic carbon.
4) The overall effective CO_2 yield after all organic carbon is consumed. Calculation of this yield includes the effective yields from the denitrifcation step and both sulfate reduction steps. The overall effective yield ranged between 0.57 and 0.62 moles of CO_2 per mole of consumed organic carbon.

Brush et al. (2006) did not include Castile brines as a source of sulfate in the EQ6 calculations because the quantity of Castile sulfate that could enter the repository is an uncertain parameter (see Section 4.2.1.2). Hence, the EEF calculation will use a modified value of the effective CO_2 yields calculated by Brush et al. (2006) to incorporate the effect of Castile brines. This modification is detailed in Section 4.2.3.

Several known calcite inhibitors are expected to be present in both the WIPP brines and waste, so Brush et al. (2006) also examined the potential inhibition of calcite precipitation. Brush et al. (2006) note that "a number of other $CaCO_3$-bearing minerals can still precipitate if the formation of calcite is inhibited. These minerals, which are metastable with respect to calcite, include aragonite ($CaCO_3$), vaterite ($CaCO_3$), monohydrocalcite ($CaCO_3 \cdot H_2O$), ikaite ($CaCO_3 \cdot 6H_2O$), and $CaCO_3$(am) (Brooks et al., 1950; Gal et al., 1996)" Brush et al. (2006) additionally state that when considering individual inhibitors, "none of them have been shown to completely inhibit the precipitation of all forms of $CaCO_3$."

The possibility that multiple inhibitors could act simultaneously on the same solution was also considered, and Brush et al. (2006) found that "while studies have shown that Mg^{2+} inhibits calcite formation (Katz, 1973) and citrate inhibits aragonite formation (Westin and Rasmuson, 2005), the simultaneous presence of Mg^{2+} and citrate can lead to the formation of so-called "magnesian calcites," $Mg_xCa_{1-x}CO_3$, where the magnesium content $x < 0.5$." Brush et al. (2006)

state that "Because aragonite formation increases with increasing Mg^{2+} concentration, it is possible that, under the conditions present in WIPP brines … aragonite could be the dominant $CaCO_3$ phase, with magnesian calcite containing up to 22% $MgCO_3$ as the secondary form of precipitated $CaCO_3$." This result is relevant to the EEF analysis because if CO_2 sequestration in the WIPP occurred via formation of magnesian calcites, magnesium from the emplaced MgO would likely be consumed.

To account for the possibility of the formation of magnesian calcites in the WIPP, this analysis will conservatively assume that any CO_2 not sequestered in hydromagnesite or magnesite in Brush et al.'s (2006) EQ6 simulations was sequestered in $Mg_xCa_{1-x}CO_3$, rather than the $CaCO_3$-bearing minerals predicted by EQ6. Furthermore, this analysis will conservatively assume that the magnesian calcite contains 22% Mg, the maximum Mg content that Brush et al. (2006) assessed could be found in WIPP magnesian-calcites. This mineral would have the formula $Mg_{0.22}Ca_{0.78}CO_3$. For calculation of the EEF, precipitation of 1 mole of $Mg_{0.22}Ca_{0.78}CO_3$ is mathematically equivalent to the coprecipitation of 0.22 moles of $MgCO_3$ and 0.78 moles of $CaCO_3$. Thus, the effective CO_2 yields calculated by Brush et al. (2006) are modified for the EEF analysis in the following manner:

4-6 $$yield = F_{mag/hydromag} + 0.22 \times F_C$$

where $F_{mag/hydromag}$ denotes the fraction of CO_2 sequestered in either magnesite or hydromagnesite and F_C denotes the fraction of CO_2 consumed by precipitation of $CaCO_3$-bearing minerals. This modification results in effective CO_2 yields that range from 0.62 to 0.69 moles of CO_2 per mole of consumed carbon when sulfate reduction proceeds with sulfate from DRZ minerals. This analysis will conservatively assume a yield of 0.69 moles of CO_2 per mole of consumed carbon when sulfate reduction proceeds with sulfate from DRZ minerals.

4.2.1.2 Quantities of Sulfate in Salado and Castile Brines

The brines in the Castile and Salado Formations are important factors for CO_2 generation by microbes. Not only do they provide the water required for microbial respiration, but they are also a potential source of sulfate for sulfate reduction.

WIPP PA uses Generic Weep Brine (GWB) and Energy Research and Development Administration (WIPP Well) 6 (ERDA-6) to simulate Salado and Castile brines, respectively. GWB is a synthetic brine typical of intergranular (grain-boundary) fluids from the Salado Formation at or near the stratigraphic horizon of the repository (Snider 2003b), and ERDA-6 is a synthetic brine representative of fluids in brine reservoirs in the Castile Formation (Popielak et al. 1983).

Table 1 lists the components of GWB and ERDA-6 prior to equilibration with MgO. The brines contain similar sulfate concentrations (approximately 0.17 M). However, the Mg^{2+} concentration in GWB is more than 50 times higher than the Mg^{2+} concentration in ERDA-6, and this difference is significant to the EEF calculation for the following reason. Even though Salado brines can provide a source of sulfate reduction, they also contain Mg^{2+} that can carbonate and sequester CO_2.

Two moles of CO_2 are generated for every mole of SO_4^{2-} that is consumed during sulfate reduction (4-4). For every mole of SO_4^{2-} in GWB, there are more than 5 moles of Mg^{2+}. Thus, Salado brines contain enough Mg^{2+} to consume more than twice as much CO_2 that could be generated when sulfate reduction consumes sulfate from Salado brines. Hence, for the purposes of calculating the EEF, it is conservative to assume Salado brines are not a significant source of sulfate[5]. The EEF will include Castile brines as a source of sulfate since their Mg^{2+} concentrations are much lower than the Salado brine Mg^{2+} concentrations.

Table 1 Compositions of GWB and ERDA-6 Before Equilibrium with MgO (M, unless otherwise noted)

Element or Property	GWB Before Reaction with MgO, Halite, and Anhydrite[A]	ERDA-6 Before Reaction with MgO, Halite, and Anhydrite [B]
$B(OH)_x^{3-x}$	0.158	0.063
Na^+	3.53	4.87
Mg^{2+}	1.02	0.019
K^+	0.467	0.097
Ca^{2+}	0.014	0.012
SO_4^{2-}	0.177	0.170
Cl^-	5.86	4.8
Br^-	0.0266	0.011
Total inorganic C	-	16 mM
Ionic strength	-	-
$\log f_{CO_2}$	-	-
pH	-	6.17
Relative humidity	-	-
Specific gravity	1.2	1.216

[A]From Snider (2003b)
[B]From Popielak et al. (1983)

In the event that a drilling intrusion into the repository intersects a pressurized brine pocket in the Castile formation below the repository, brine could possibly flow into the repository and transport quantities of dissolved sulfate into contact with the waste materials. Clayton and Nemer (2006) conducted an analysis to calculate a probability distribution for the amount of sulfate in Castile brines that could enter the waste areas during the 10,000 year regulatory time period. In this analysis, a Monte Carlo simulation was used to generate 1,000 distinct repository drilling-event futures. These futures contain sequences of drilling intrusions that penetrate the repository. For each future, the "worst case" panel with the most E1 intrusions was identified. Since only an E1 intrusion (an intrusion that intersects a Castile brine pocket and is plugged with a type 2 borehole plug) will allow Castile brine to enter the repository, the "worst case" panel for a given future is the panel that has the most E1 intrusions in that future and, hence, has the greatest quantity of Castile sulfate. Additionally, CRA-2004 PABC BRAGFLO results (Nemer and Stein 2005) were used to calculate a distribution of quantities of Castile sulfate that could

---

[5] The analysis by Brush et al. (2006) discussed in Section 4.2.1.1 does not ignore the sulfate content in Salado brines.

enter an intruded panel from a single E1 intrusion. Finally, the uncertainties in the drilling futures were combined with the uncertainties in the Castile sulfate quantities to create a probability distribution of quantities of sulfate from Castile brines that could enter the "worst case" panel over the 10,000 year regulatory time period.

Figure 1 shows the complementary cumulative distribution function (CCDF) for the quantities of Castile sulfate that could enter the "worst case" panel over the 10,000 year regulatory time period. In this figure, the "yield of Castile sulfate" indicates the fraction of the organic carbon that can be consumed via sulfate reduction with Castile sulfate. On average, 2.4 mole % of the organic carbon in the "worst case" panel could be consumed via sulfate reduction with Castile sulfate. This mean percentage is fairly small because almost 30% of the drilling futures have no E1 intrusions, and consequently, no Castile sulfate enters any of the panels in these futures. The standard deviation of the distribution of the quantities of Castile sulfate that could enter the "worst case" panel over the 10,000 year regulatory time period is 5.1 mole %.
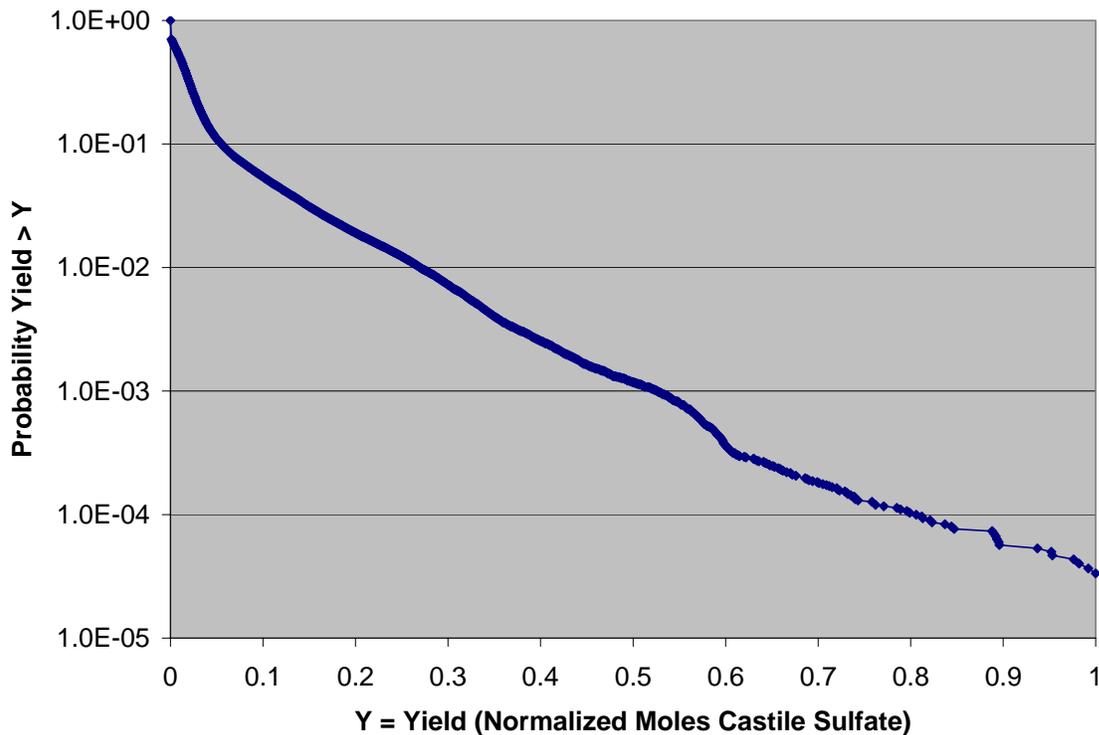
Figure 1 CCDF of Normalized Moles of Castile Sulfate that enter the "Worst Case" Waste Panel (Figure 1 from Clayton and Nemer (2006))

4.2.2 Methanogenesis

As mentioned in Section 4.2, denitrification and sulfate reduction are preferential microbial respiration pathways when compared to methanogenesis. However, if neither nitrates nor sulfates are available, microbial respiration can only proceed via methanogenesis. The fraction of organic carbon in the repository that is consumed via methanogenesis is relevant to EEF calculations because methanogenesis results in 0.5 moles of CO_2 per mole of consumed carbon, as opposed to 1.0 moles per mole of consumed carbon from denitrification and sulfate reduction (without including the effects of calcite precipitation).

Kanney et al. (2004) conducted an analysis that attempted to bound the quantities of sulfate that could enter the disposal rooms by diffusive and advective transport mechanisms. Despite the conservative nature of that analysis, the results indicated that the quantities of sulfate entering the repository due to advective transport of sulfate in the event of a human intrusion or diffusive transport of sulfate in the undisturbed scenario do not preclude methanogenesis.

However, the EPA stated that the analysis by Kanney et al. (2004) did not "adequately address all sources of natural sulfate that could be available to the repository" (EPA 2004a). EPA questioned the rate of DRZ healing and fracturing discussed in the Kanney et al. (2004) analysis and postulated that a significant quantity of sulfate could be introduced into disposal rooms in the event of room collapse (EPA 2004a). The EPA concluded that the Kanney et al. (2004) analysis did not adequately bound the quantity of sulfate that could enter the repository (EPA 2004a) and directed that WIPP PA conservatively assume that only denitrification and sulfate reduction be considered as viable microbial respiration pathways for CO_2 generation for the CRA-2004 PABC (Cotsworth 2005).

The analysis herein does not attempt to derive a conservative bound on the total amount of sulfate that could enter the repository. Rather, it acknowledges that there is some uncertainty in the quantity of sulfate that could enter the repository and, hence, uncertainty in the fraction of the organic carbon in the emplaced CPR materials that could be consumed via methanogenesis. This uncertainty has not been quantified to date. The following section discusses how uncertainties related to methanogenesis are handled for the EEF calculation.

4.2.3 CO_2 Yield

The effective CO_2 yields that Brush et al. (2006) calculated did not include Castile brines as a source of sulfate in the EQ6 calculations because the quantity of Castile sulfate that could enter the repository is an uncertain parameter. This section details the calculation of the overall effective CO_2 yield by incorporating the results from Brush et al. (2006) with the quantification of Castile sulfate in the repository by Clayton and Nemer (2006)

Equation 4-7 indicates how the effective CO_2 yield, y_{yield}, is calculated:

4-7
$$y_{yield} = \left(F_D + F_{SW} + F_{SC}\right) \times \frac{1 \text{ mole } CO_2}{1 \text{ mole consumed C}}$$
$$+ F_{SM} \times \frac{0.69 \text{ mole } CO_2}{1 \text{ mole consumed C}} + F_M \times \frac{0.5 \text{ mole } CO_2}{1 \text{ mole consumed C}}.$$

F_D denotes the fraction of carbon consumed via denitrification, F_{SW} denotes the fraction consumed via sulfate reduction using sulfate from the waste materials, F_{SC} denotes the fraction consumed via sulfate reduction using Castile sulfate, F_{SM} denotes the fraction consumed via sulfate reduction using sulfate from DRZ minerals, and F_M denotes the fraction consumed by methanogenesis.

As discussed in Section 4.2.2, the uncertainty in the fraction of the organic carbon in the emplaced CPR materials that could be consumed via methanogenesis cannot be presently quantified. For this reason, the calculation of y_{yield} will conservatively assume that organic carbon will not be consumed via methanogenesis. The following factors are considered when calculating y_{yield}:

1) All of the organic carbon in the emplaced CPR materials will be consumed during the 10,000 year regulatory time period.
2) 4.89 mole % of the carbon in the CPR materials is consumed via denitrification, i.e. $F_D = 0.0489$.
3) The other 95.11 mole % of carbon in the CPR materials is consumed via sulfate reduction. It is conservatively assumed that no carbon is consumed by methanogenesis, i.e. $F_M = 0$.
4) 0.84 mole % of the carbon in the CPR materials is consumed via sulfate reduction using sulfate from the waste materials, i.e. $F_{SW} = 0.0084$.
5) It is conservatively assumed that sulfate reduction will preferentially use sulfate from waste materials and Castile brines before sulfate from surrounding minerals. This assumption is conservative because sulfate reduction with sulfate from waste materials and Castile brines has a higher CO_2 yield than sulfate reduction with sulfate from the surrounding minerals.

Issue 5) leads to the following constraint:

4-8
$$F_{SM} = 1 - \left(F_D + F_{SW} + F_{SC}\right).$$

Based upon the above factors and Eq. 4-8, Eq. 4-7 can be simplified in the following manner:

4-9
$$y_{yield} = \frac{0.708 \text{ mole } CO_2}{1 \text{ mole consumed C}} + F_{SC} \times \frac{0.31 \text{ mole } CO_2}{1 \text{ mole consumed C}}.$$

Recall from Section 4.2.1.2 that Clayton and Nemer (2006) developed a probability distribution for the fraction of carbon that could be consumed by sulfate reduction with Castile sulfate, and this distribution had a mean value of 0.024 and standard deviation of 0.051. By assuming that F_{SC} has that same mean and standard deviation, then y_{yield} is a random variable with a mean, μ_{yield}, of 0.715 moles of CO_2 per mole of consumed carbon and a standard deviation, σ_{yield}, of 0.0158 moles of CO_2 per mole of consumed carbon.

Before concluding the discussion of the CO_2 yield, it is prudent to assess what impact inclusion of methanogenesis would have on the calculation of y_{yield}. Inclusion of this uncertainty would increase σ_{yield} and decrease μ_{yield} because the CO_2 yield from methanogenesis (0.5 moles of CO_2 per mole of consumed carbon) is lower than any of the yields from the other microbial respiration. In fact, a lower bound on μ_{yield} could be estimated by assuming that the waste materials are the only source of sulfate for sulfate reduction. Consequently, if all of the organic carbon in the emplaced CPR materials were consumed, 4.89 mole % of the carbon would be consumed via denitrification, 0.84 mole % by sulfate reduction, and 94.27 mole % by methanogenesis, and the effective CO_2 yield would be 0.53 moles of CO_2 per mole of consumed carbon.

However, the EEF calculation will assume that methanogenesis will not occur in the repository, and, thus, μ_{yield} equals 0.715 moles of CO_2 per mole of consumed carbon and σ_{yield} equals 0.00158 moles of CO_2 per mole of consumed carbon.

4.3   *Random Variables Affecting CO_2 Production*

As in Eq. 4-2, the quantity (in moles) of CO_2 produced by microbial respiration is the product of the random variables y_{yield} and y_{CPR} and the moles of carbon in the emplaced CPR materials, M_C. Since this product represents the denominator in the EEF calculation ($g \times M_C$ in Eq. 3-2), these two terms can be equated to define the random variable g:

4-10
$$g = y_{yield} \times y_{CPR}.$$

This calculation makes the following assumptions:
1) All of the organic carbon in the emplaced CPR materials is consumed.
2) None of the organic carbon in the CPR materials is consumed via methanogenesis.

5.0 Quantities of MgO Available for Reaction

The numerator in the EEF calculation represents the amount of MgO that is available to sequester CO_2. This quantity is represented in the EEF calculation as the product of the number of moles of emplaced MgO (M_{MgO}) and a random variable, m, that represents the percentage of the emplaced moles that are available for reaction (Eq. 5-1).

5-1
$$\text{available moles of MgO} = m \times M_{MgO}$$

Several uncertainties have the potential to impact the random variable m, and these uncertainties are grouped into two categories: issues related to MgO characteristics and performance and issues related to the repository characteristics and performance. The individual uncertainties associated with these categories and their impacts on the random variable m are detailed in Sections 5.1 and 5.2.

5.1   *MgO Characteristics and Performance*

Three issues that are related to characteristics of MgO and its performance and could potentially affect the amount of MgO available for reaction have been identified. They are:
1) the concentration of reactive constituents in MgO;
2) the possibility of carbonation of periclase prior to emplacement; and
3) the extent of the reaction of MgO with CO_2.

5.1.1 Reactive Constituents in MgO

Brush and Roselle (2006) reviewed a set of previously conducted experiments that were conducted to assess the concentration of reactive constituents in the MgO that is emplaced in the repository. Brush and Roselle (2006) present results for MgO from two of the three vendors that have supplied WIPP with MgO. Because a reduction in the EF would only affect quantities of MgO from the current supplier and not previous suppliers, this analysis restricts discussion to the MgO received from the current supplier.

The current provider of MgO for the WIPP is Martin Marietta Magnesia Specialties LLC. The main reactive constituent of MgO is periclase, pure crystalline MgO, and lime (CaO), another reactive constituent, is also expected to be found in the emplaced MgO. Table 2 shows the results from a "loss on ignition" (LOI) experiment to assess the concentration of reactive constituents in two MgO materials from Martin Marietta, MagChem 10 WTS-20 and MagChem 10 WTS-60. ("MagChem 10" is omitted hereafter.) WTS-60 is the material that is currently being emplaced in the repository.

Brush and Roselle (2006) state that

> *LOI at 750 ºC yields higher brucite and portlandite contents (and, by assumption, higher initial periclase and lime contents) than LOI at 500 ºC …LOI at 750 ºC was unsuccessful for WTS-20 and WTS-60 due to decrepitation of these samples at this temperature. Wall (2005) was unable to develop a procedure for LOI at 750 ºC that prevented decrepitation of these samples. However, the fact that LOI for WTS-60 at 500 ºC yielded a higher brucite and portlandite content than LOI with WTS-30 at this temperature strongly suggested that the sample of WTS-60 tested by Wall (2005) had a periclase and lime content greater than or equal to that of WTS-30, and that the brucite and portlandite content of WTS-60 from LOI at 750 ºC would equal or exceed 96 mol %, or 97 wt % (see* [Table 2]*). Therefore, it seemed reasonable to conclude that WTS-60, the MgO that is currently being emplaced in the WIPP, contains 96 mol % (97 wt %) periclase and lime.*

Brush and Roselle (2006) describe another MgO study by Deng et al. (2006a) that has quantified the concentration of reactive constituents in WTS-60. Brush and Roselle (2006) write the following:

> *Deng et al. (2006b) conducted chemical, and LOI and thermal gravimetric (TGA) analyses of WTS-60. They analyzed for Mg, Ca, Al, Fe, and Si by gravimetric determination of SiO_2, which involved: (1) dissolution in nitric acid, (2) analysis of the liquid by ICP-AES, and (3) weighing the*

> *remaining solids (Deng et al, 2006b, Appendix B, Subsection B.1). They*
> *performed LOI and TGA by determining the weight percent of H_2O*
> *released by hydrated MgO from 150-800 ºC and assuming that*
> *nonreactive components do not hydrate to a significant extent and that any*
> *unbound water will be lost at temperatures below 150 °C (Deng et al.,*
> *2006b, Appendix B, Subsection B.2).*

Deng et al. (2006b) conclude that the mean mole fraction of periclase plus lime in WTS-60 is 96% and the standard deviation of that mole fraction is 2%.

Thus, the concentration of reactive constituents in WTS-60 was calculated using two different methods, and both analyses concluded that the mean mole fraction of periclase and lime in WTS-60 was 96 %. These corroborating analyses provide confidence that the concentration of reactive constituents has accurately been calculated. Thus, the random variable y_{RC} will be used to represent the uncertainty in the concentration of reactive constituents in the emplaced MgO, and y_{RC} will be assigned a mean of 0.96 (μ_{RC} =0.96) and standard deviation of 0.02 (σ_{RC} =0.02).

Table 2 Effects of Temperature Used for LOI Analysis of MgO Hydration Products on the Brucite + Portlandite Contents of the Samples (Excerpted from Wall (2005), Table 1).

	Temperature Used for LOI			
	500 ºC		750 ºC	
Material	Mole %[1]	Wt %[1]	Mole %[1]	Wt %[1]
WTS-30	87 ± 5	91 ± 4	96 ± 5	97 ± 3
WTS-60	90 ± 3	93 ± 2	ND	ND

[1]Uncertainties reported represent two standard deviations.

5.1.2 Carbonation of Periclase Prior to Emplacement in the WIPP

During the original WIPP certification, EPA asked for "evidence that CO_2 would not diffuse through or otherwise penetrate the bags during the operational phase and reduce the post-closure capability of the MgO" (DOE 1997). DOE provided an analysis demonstrating less than 0.1% of the MgO would be lost from CO_2 penetrating the bag over 30 years. Later, the EPA asked the same question during the recertification as comment C-23-12 (EPA 2004b). DOE responded to this question in their 6th response submittal (DOE 2004b) by referencing the CCA response and providing information on the MgO supersack specification. The specification requires the supersack to be "equivalent to or better than…a standard commercial cement bag" to ensure that the supersack will effectively prevent atmospheric CO_2 and H_2O from reacting with the periclase and lime prior to creep closure of the repository and concomitant rupture of the supersacks. This analysis will conservatively assume that, due to carbonation of periclase prior to emplacement, 0.1% of the emplaced MgO will be unavailable to sequester CO_2 after closure of the repository.

5.1.3 Expected Extent of Reaction of Periclase and/or Brucite with CO$_2$

Brush and Roselle (2006) reviewed a set of experiments that were conducted to "determine whether lithification [i.e. "caking"] of MgO will occur in the WIPP and, if so, whether it would affect the rate of hydration of MgO." Brush and Roselle (2006) state that it can be said that all results to date - either from studies carried out for the WIPP Project or those for other applications - imply that the periclase present in MgO will continue to react until all CO$_2$ is consumed." Brush and Roselle (2006) further note, however, that "proving that a process will not occur in 10,000 years is very difficult."

This analysis will assume that all of the periclase will be available to react and will continue to react until all of the CO$_2$ is consumed. However, because the uncertainty in this assumption cannot be fully quantified, it will not be included in calculation of the EEF. If it was possible to quantify this uncertainty and the uncertainty was included in calculation of the EEF, it would have the potential impact of decreasing the mean EEF and increasing the standard deviation. The magnitudes of these changes are expected to be small.

5.2 *Repository Characteristics and Performance*

Five issues that are related to characteristics of the repository and its performance and could potentially affect the amount of MgO available for reaction have been identified. They are:
1) the likelihood that the MgO supersacks will rupture making MgO available to sequester CO$_2$;
2) the loss of dissolved MgO out of waste areas due to brine outflow;
3) the mass of MgO in individual supersacks;
4) the probability that CO$_2$ will be able to be transported to MgO for sequestration via brine mixing processes; and
5) physical segregation of MgO from CO$_2$.

5.2.1 Likelihood of Supersack Rupture

There are two primary mechanisms that are expected to cause supersack rupture. In DOE's March 8, 2005 letter to Bonnie Gitlin of the EPA (DOE 2005), DOE stated that microbial biodegradation would provide the failure mechanism for the MgO supersacks. This is a reasonable argument because additional quantities of MgO will only be needed in those situations where plastic and rubber materials are expected to degrade by microbial action. It is consistent with this analysis to conclude that microbial action will provide the failure mechanism for supersack rupture because this analysis assumes that all of the organic carbon in the emplaced CPR materials (including the MgO supersack bags) will be consumed

Hansen (2005) also addressed the issue of supersack rupture. Hansen (2005) stated that

> "*approximate bearing stress over the area of the* [supersack] *at the point of rupture is about six pounds per square inch (6 psi). The vertical stress that the creeping salt will apply to the waste stack will approach the lithostatic pressure of approximately 2000 psi, a stress that is hundreds of times greater than the*

maximal loading specifications for super sack rupture. This calculation is an example of an ideal loading condition. The actual features of the underground would most likely cut, puncture or tear the fabric before salt creep imparts significant compressive load to the bags."

Thus, this analysis assumes that all MgO supersacks will rupture due to either microbial degradation or lithostatic loading, making the MgO available for consumption of CO_2.

5.2.2 Loss of MgO to Brine Outflow

MgO that has dissolved in brine may possibly leave the waste areas before reacting with CO_2 when brine flows out of the repository (Clayton and Nemer 2006). This process is termed the "loss of MgO to brine outflow" in this analysis.

Using a procedure similar to that described in Section 4.2.1, Clayton and Nemer (2006) conducted a Monte Carlo analysis to calculate the probability distribution for the fraction of MgO that could be lost due to brine outflow during the 10,000 year regulatory time period. This analysis incorporated brine outflow results from the CRA-2004 PABC analysis with a Monte Carlo simulation of 1,000 possible drilling futures. Under the assumption that DOE uses an MgO EF of 1.2 for MgO emplacement, Clayton and Nemer (2006) concluded that on average, 0.008 of the emplaced MgO would be lost due to brine outflow. The standard deviation for the distribution of the fraction of MgO lost due to brine outflow is 0.019. Figure 2 shows the CCDF for the fraction of MgO lost due to brine outflow.

The random variable y_{L2B} will be used to represent the uncertainty in the fraction of MgO lost due to brine outflow, and y_{L2B} will be assigned a mean of 0.008 (μ_{L2B} =0.008) and standard deviation of 0.019 (σ_{L2B} =0.019).
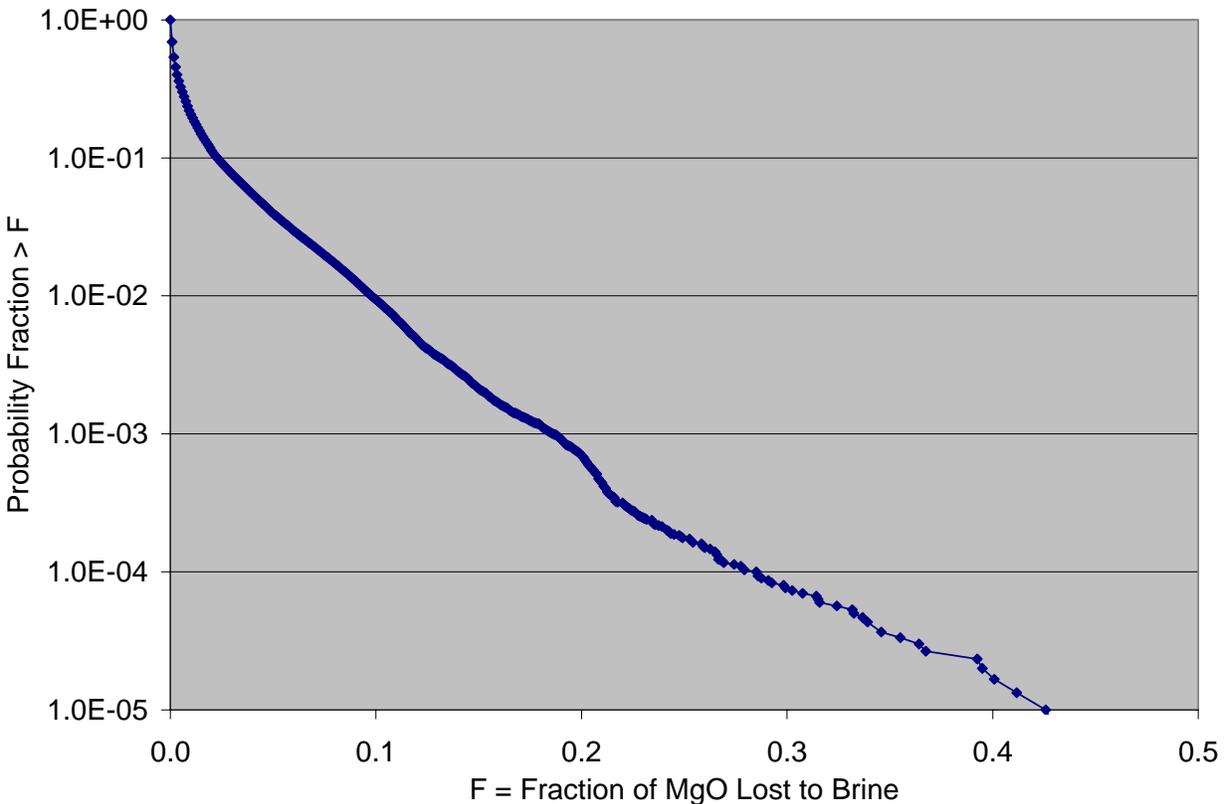
Figure 2 CCDF for the Fraction of MgO Lost to Brine Outflow

5.2.3 Mixing Processes

As part of DOE's MgO mini-sack removal analysis, Wang (2000) analyzed diffusion processes in the repository. Wang (2000) concluded that diffusion processes alone are sufficient to mix CO_2 with WIPP brines over length scales corresponding to final room height, during time scales corresponding to maximum average brine flows.

The analysis of Wang (2000) was updated by Kanney and Vugrin (2006) for conditions that reflect the CRA-2004 PA Baseline Calculation (PABC) technical baseline. The conclusions of Wang (2000) did not change for the new technical baseline.

Furthermore, to address the EPA's concern that emplacement of supercompacted waste could affect MgO effectiveness (Gitlin 2006), Kanney and Vugrin (2006) applied the analysis of Wang (2000) in a modified form to the results of the Advanced Mixed Waste Treatment Project (AMWTP) analysis performed by Hansen et al. (2004). The conclusions drawn in Wang (2000) were not impacted by supercompacted waste and heterogeneous waste emplacement.

It should be noted that the analysis of Kanney and Vugrin (2006) does not include gaseous diffusion of CO_2 throughout a room. Because the rate of gaseous diffusion of CO_2 is orders of magnitude faster than aqueous diffusion, gaseous diffusion of CO_2 is very rapid and will maintain uniform conditions in the areas in a room above the brine when a diffusion pathway

exists. Thus, the analysis of Wang (2000) and Kanney and Vugrin (2006) can be considered conservative because gaseous diffusion is not considered.

Additionally, under most flow conditions, mixing rates due to advection and dispersion should dominate over molecular diffusion, and since Kanney and Vugrin (2006) do not include these mixing mechanisms in their analysis, these results indicate that one should have a high level of confidence that sufficient mixing will occur throughout the regulatory period. Thus, this analysis will assume that the mixing processes expected in the repository will be sufficient to maintain a well-mixed brine.

5.2.4 Physical Segregation of MgO

Physical segregation of a quantity of MgO from brine or CO_2 due to roof collapse could potentially impact the quantity of MgO available to sequester CO_2; however, the probability of this segregation and the potential impact is negligible. It is probable that any roof failure will occur by lowering of a roof beam onto the waste/MgO stack so that the failed material will not intrude into the stack. Secondly, any failed roof which might occur in smaller blocks will be fractured and will maintain a fairly high permeability to brine and gas for a significant amount of time. Finally, any small scale spalling of the roof into the interstices of the stacks will also probably maintain a high permeability either because grains will not re-cement easily, or if they do, they will form a coherent mass with brine, MgO, and gas outside of them.

Furthermore, the current method that DOE uses to emplace the MgO and calculation of the MgO excess factor on a room basis likely minimizes the possible physical segregation of MgO from brine and CO_2. Operational controls guarantee one MgO supersack is emplaced on each stack of waste. If this quantity is not sufficient to meet the required MgO EF for a room, additional MgO is emplaced. These EPA audited operations are detailed in WIPP technical procedures (WTS 2006).

Thus, no MgO is expected to be unavailable due to physical segregation, and this analysis will assume such. The uncertainty with this assumption cannot presently be quantified, so the uncertainty will not be included in EEF calculations. If it was possible to quantify this uncertainty and the uncertainty was included in calculation of the EEF, it would have the potential impact of decreasing the mean EEF and increasing the standard deviation. The magnitudes of these changes are expected to be small.

5.2.5 Mass of MgO in a Supersack

The uncertainty in the mass of MgO per supersack is controlled by the procurement specification on MgO. The specification requires that each supersack must weigh 4,200 pounds, plus or minus 50 pounds (WTS 2005). The uncertainty of MgO in an individual supersack contributes to the uncertainty in the mass of MgO in a room.

Mood et al. (1974) give the following results that are used to calculate the uncertainty in the mass of MgO in a single room:

Let $X_{total} = \sum\limits_{i=1}^{n} X_i$, where X_i are elements of the same population having mean

μ and standard deviation σ and that their measurement is free from bias. Then

5-2
$$X_{total} = n\mu$$

and

5-3
$$\sigma_{total} = \sigma(X_{total}) = \sigma\sqrt{n}.$$

Thus the relative variability, or coefficient of variation (CV), for the total is

5-4
$$CV = \frac{\sigma_{total}}{X_{total}} = \frac{\sigma}{\mu\sqrt{n}}.$$

The masses of MgO in a supersack are expected to be independent and free from bias, so the above result from Mood et al. (1974) can be used to calculate the uncertainty in the total mass in the entire room.

Vugrin (2006) indicates that the number of supersacks per room in Panel 2 and closed rooms in Panel 3 (rooms 4, 5, 6, 7) ranges between 363 and 540 supersacks[6]. The number of supersacks per room for an EF of 1.2 is estimated to range between 260 and 388 ($363 \times 1.2/1.67 = 260$ and $540 \times 1.2/1.67 = 388$). By conservatively using the low end of the range of supersacks per room, the relative variability in mass of MgO in a room is calculated to be 0.00037 (Eq. 5-5). A standard deviation of 25 pounds is used since it is assumed that the possible 50 pound deviation from 4,200 pounds in the procurement specification represents two standard deviations.

5-5
$$\frac{\sigma_{Total}}{X_{Total}} = \frac{25}{4200\sqrt{260}} = 0.00037.$$

Because the moles of emplaced MgO are multiplied by the random variable m in the numerator of the EEF calculation (Eq. 3-2), it is necessary to know uncertainty in the amount of MgO present in the repository relative to the amount that DOE tracks. Since the DOE takes credit for 4,200 lbs of MgO for each supersack that is emplaced, regardless of the variability of masses in the individual supersacks, the expected mass of MgO in a room, X_{Total}, is equal to the mass of MgO for which the DOE takes credit. Thus, the ratio of these two quantities is 1. The relative uncertainty, as calculated in Eq. 5-5, is 0.00037. This analysis will use the random variable y_{SS} to represent the uncertainty in the amount of MgO present in the repository relative to the amount that DOE tracks, and this random variable will have a mean value of 1 ($\mu_{SS} = 1$) and standard deviation 0.00037 ($\sigma_{SS} = 0.00037$).

---

[6] Because some rooms in Panel 1 were not completely filled, only the rooms in Panels 2 and 3 are used to determine the expected number of supersacks per room.

5.3 *Random Variables Affecting MgO Availability*

Based upon the preceding discussion in Sections 5.1 and 5.2, the moles of MgO available for sequestration of CO_2 can be calculated as follows:

5-6
$$\text{moles of available MgO} = y_{SS} \times y_{RC} \times 0.999 \times M_{MgO} - y_{L2B} \times M_{MgO}$$

5-7
$$= \left(y_{SS} \times y_{RC} \times 0.999 - y_{L2B} \right) \times M_{MgO}$$

where the random variable y_{SS} represents the uncertainty in the amount of MgO present in the repository relative to the amount that DOE tracks, y_{RC} is a random variable representing the uncertainty in the concentration of reactive constituents in MgO, and y_{L2B} is a random variable representing the fraction of MgO lost to brine outflow. Since Eq. 5-7 represents the numerator in the EEF, equating the right-hand side of Eq. 5-7 with the right-hand side of Eq. 5-1 yields the following definition of the random variable m:

5-8
$$m = y_{SS} \times y_{RC} \times 0.999 - y_{L2B}.$$

This calculation makes the following five assumptions:
1) All of the periclase in the MgO will be available to react and will continue to react until all of the CO_2 is consumed.
2) 0.1% of the periclase in the MgO will carbonate prior to emplacement and, thus, be unavailable to sequester CO_2 after closure of the repository. (Hence, the multiplicative 0.999 factor in Eq. 5-8).
3) All MgO supersacks will rupture, making MgO available for consumption of CO_2.
4) The mixing processes expected in the repository will be sufficient to maintain a well-mixed brine.
5) No MgO is rendered unavailable for CO_2 consumption due to physical segregation.

6.0 Consumption of CO_2 by MgO and Other Repository Features

The variable r in Eq. 3-2 represents the uncertainty in the moles of CO_2 that an individual mole of MgO will consume. Four issues affecting this uncertainty have been identified:
1) consumption of CO_2 by hydromagnesite and magnesite;
2) consumption of CO_2 by materials other than MgO;
3) dissolution of CO_2 in WIPP brines; and
4) incorporation of CO_2 in biomass.
These uncertainties are discussed in the following sections.

6.1 *Hydromagnesite and Magnesite*

When brucite reacts and consumes CO_2, hydromagnesite is formed. The subsequent conversion of hydromagnesite to magnesite returns magnesium which can consume additional CO_2. The number of moles of CO_2 sequestered per mole of magnesium is different for hydromagnesite and magnesite, and thus has the potential to impact the EEF calculation. Furthermore, the rate of magnesite formation relative to CO_2 production could potentially impact the EEF calculation. This section analyzes these two factors. Brush and Roselle (2006) state that if CO_2 is present in the repository, MgO will continue to react until all of the CO_2 is consumed (Section 5.1.3), so

this portion of the analysis only addresses whether or not enough MgO will be present to consume all of the CO_2 that could be generated.

The differential equations governing the production of hydromagnesite and its eventual conversion to magnesite are the CO_2 production equation,

6-1
$$\frac{dCO_2}{dt} = k_{CO2},$$

and the hydromagnesite production equation,

6-2
$$\frac{dhymag}{dt} = \frac{1}{4} k_{CO2} - k_{mag}(hymag).$$

Here k_{CO2} is the zeroth order rate of microbial CO_2 production, 4 moles of CO_2 are used to produce one mole of hydromagnesite (Eq. 5 in Brush and Roselle (2006)), and k_{mag} is the first order rate constant for hydromagnesite conversion to magnesite. In writing Eq. 6-1, it is assumed that CO_2 production is zeroth order, and this assumption is consistent with how CO_2 production is modeled in WIPP PA. In Eq. 6-2 it is assumed that on the timescale of interest, CO_2 production is the time-controlling step for hydromagnesite production, and that the conversion of hydromagnesite to magnesite is a first order reaction (Brush and Roselle 2006). Eq. 6-3 shows the brucite carbonation reaction that produces hydromagnesite (Brush and Roselle 2006).

6-3
$$5Mg(OH)_2 + 4CO_2(aq \text{ or } g) \quad Mg_5(CO_3)_4(OH)_2 \cdot 4H_2O$$

Given Eqs. 6-1, 6-2, and 6-3, the equation for the amount of uncarbonated magnesium in the system is written as follows,

6-4
$$\frac{dMg_{uncarb}}{dt} = -\frac{5}{4} k_{CO2} + k_{mag}(hymag).$$

In Eq. 6-4, the production of hydromagnesite consumes 5 moles of magnesium for every 4 moles of CO_2 (Eq. 6-3), and the conversion of hydromagnesite to magnesite produces one mole of brucite. Solving Eqs. 6-1, 6-2, 6-4 for the amount of uncarbonated magnesium yields,

6-5
$$Mg_{uncarb} = \left(Mg_{uncarb,t=0} - \frac{1}{4}\frac{k_{CO2}}{k_{mag}} \right) - k_{CO2}t + \frac{1}{4}\frac{k_{CO2}}{k_{mag}} e^{-k_{mag}t}.$$

To calculate the amount of uncarbonated magnesium versus time from Eq. 6-5, the rates are needed as is the initial amount of magnesium. The maximum inundated rate of CO_2 production (WAS_AREA:GRATMICI) used in WIPP PA is 5.6×10^{-10} moles CO_2/(kg of cellulose equivalent * sec). Given that the mass of cellulose equivalents is at most 3.0×10^7 kg in the CRA-2004 PABC PA (Appendix A, Nemer and Stein (2005)) and 3.2×10^7 sec/year (REFCON:YRSEC),

$$k_{CO2} = 5.6 \times 10^{-10} \frac{mol\ CO_2}{kg\ cellulose\ equivalent\ sec} \times 3.0 \times 10^7\ kg\ cellulose\ equivalent$$

6-6

$$\times 3.2 \times 10^7 \frac{sec}{year} = 5.4 \times 10^5 \frac{mol\ CO_2}{year}$$

It should be noted that since WIPP PA assumes that one mole of CO_2 is produced for every mole of consumed organic carbon and does not include the results discussed in Section 4.2.1.1, the calculation of this rate is conservative. Use of a smaller CO_2 yield would decrease k_{CO2}. From page 13 of Brush and Roselle (2006), the half life for the conversion of hydromagnesite to magnesite in GWB is estimated to be 73 years. The induction period is estimated at 200 years. Conservatively adding these two time periods as the half life for the conversion of hydromagnesite to magnesite, and converting to a first order rate constant yields

6-7
$$k_{mag} = \frac{-\ln(1/2)}{t_{1/2}} = \frac{0.69}{273\ years} = 2.5 \times 10^{-3}\ years^{-1}.$$

Given 1.10×10^9 moles of organic carbon in the repository (Appendix A, Nemer and Stein (2005)), the time required to consume all the CPR in the inventory at the maximum rate is 2,000 years (Eq. 6-8).

6-8
$$t_{all\ CPR} = 1.1 \times 10^9\ mol\ C \bigg/ 5.4 \times 10^5 \frac{mol\ CO_2}{year} = 2 \times 10^3\ years.$$

Given an excess factor of 1.2 and 1.1×10^9 moles carbon in the inventory, the initial moles of Mg in the system is

6-9
$$Mg_{uncarb,t=0} = 1.2 \times 1.1 \times 10^9\ mol\ Mg.$$

Eqs. 6-5 through 6-9 are used to plot, in Figure 3, the fraction of uncarbonated magnesium remaining ($Mg_{uncarb}/Mg_{uncarb,t=0}$) versus the fraction of CPR consumed (time/$t_{all\ CPR}$). As shown in Figure 3, with an EF of 1.2, there is always uncarbonated magnesium remaining, approximately 15% of the emplaced Mg, when all of the CPR is consumed.

In fact, as long as the half life for the conversion of hydromagnesite to magnesite is less than 3,000 years, uncarbonated Mg will remain. Figure 4 shows the fraction of uncarbonated magnesium at 2,000 years as a function of the half life. If the half life was increased from 273 years to 500 years, approximately 10% of the emplaced Mg would remain uncarbonated after 2,000 years, and if the half life was further increased to 1,000 years, 5% of the emplaced Mg would remain uncarbonated after all of the organic carbon has been consumed. Thus, as long as the half life is less than 3,000 years, uncarbonated Mg will remain even when the maximum CO_2 production rate is used and when it is conservatively assumed that 1 mole of CO_2 is produced for every mole of consumed organic carbon.
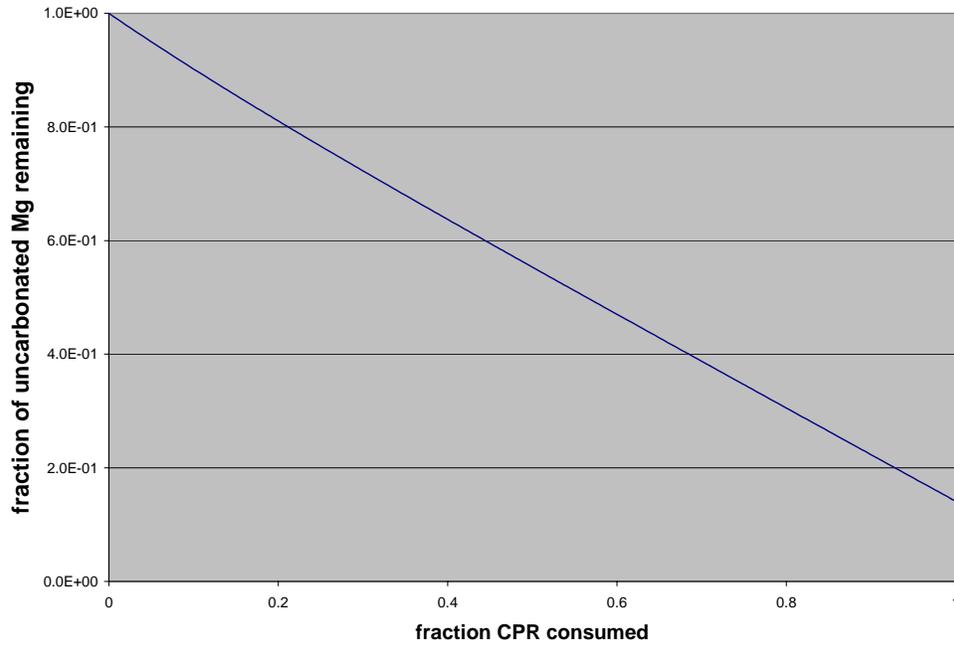
Figure 3 Fraction of Uncarbonated Mg Remaining Versus Fraction of CPR Consumed
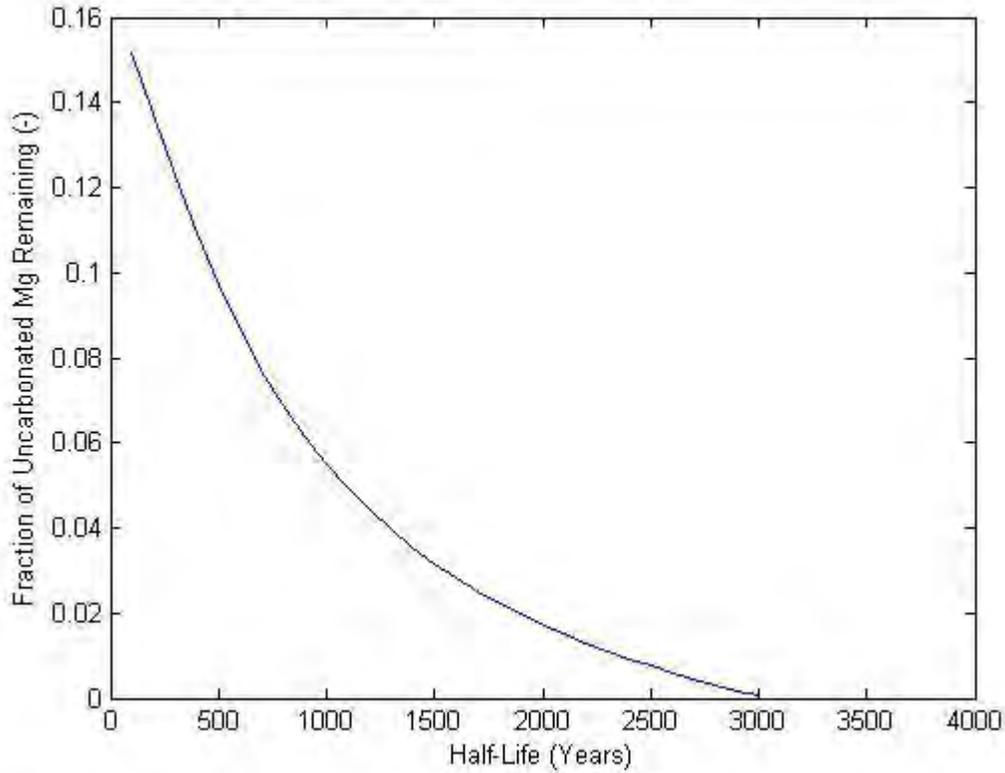
Figure 4 Fraction of Uncarbonated Mg Remaining at 2000 Years Versus the Half Life for the Conversion of Hydromagnesite to Magnesite

6.2   *Consumption of CO$_2$ by materials other than MgO*

Brush and Roselle (2006) identify four types of materials that could consume CO$_2$ (in addition to the MgO engineered barrier):

1) Fe-base metals in steel waste containers and in the TRU waste being emplaced in the repository, and the corrosion products of these metals;

2) Pb-base metals in the waste, and their corrosion products;

3) lime and portlandite in portland cements associated mainly with process sludges in the waste; and

4) dissolved Ca species that would be produced in significant quantities in Ca- and SO$_4^{2-}$-bearing minerals such as anhydrite, gypsum, and polyhalite.

Brush and Roselle (2006) state that "It is likely that these processes will consume significant amounts of CO$_2$ in addition to that consumed by MgO." Consumption of CO$_2$ by these materials is important because of the impact that they could have on the EEF calculation and chemical conditions in the repository.

The possible consumption of CO$_2$ by dissolved Ca species has already been discussed in Section 4.2.1. Brush and Roselle (2006) note that inclusion of the effects of CO$_2$ consumption by the other materials "would be difficult because of the uncertainties associated with these processes. However, these materials could consume 36.1, 1.36, and 0.177% of the CO$_2$ that would be produced by complete microbial consumption of all CPR materials." Because of these uncertainties, this analysis will use the conservative assumption that CO$_2$ will not be consumed by Fe-base metals or their corrosion products, Pb-base metals or their corrosion products, or lime and portlandite in portland cements. However, if it were possible to quantify the expected quantities of CO$_2$ that would be consumed by these materials and the associated uncertainty in calculation of the EEF, it would increase the mean EEF and possibly the EEF uncertainty. The magnitude of these increases is not known.

6.3   *Dissolution of CO$_2$ in WIPP Brines*

Brush and Roselle (2006) state that "Dissolution of CO$_2$ in WIPP brines cannot consume significant quantities of CO$_2$ relative to the quantity that would be produced by microbial consumption of all CPR materials in the repository. This is because the solubility of CO$_2$ in brines is too low, and the volumes of brines that could flow through the repository are too low to dissolve significant amounts of CO$_2$." In fact, Brush and Roselle (2006) conclude that 1,000,000 m^3 of ERDA-6[7] would contain less than 0.04% of "the total quantity of CO$_2$ that would be produced by microbial consumption of all CPR materials in the repository." For the sake of comparison, it is worth noting that the total volume of the empty waste panels in the WIPP is less than 500,000 m^3.

Because the quantities of CO$_2$ dissolved in WIPP brines will be so small relative to the quantity that would be produced by microbial consumption of all CPR materials in the repository, this

---

[7] ERDA-6 is a synthetic brine representative of fluids in brine reservoirs in the Castile Formation (Popielak et al., 1983)

factor will have little or no impact on EEF calculations. Hence, this analysis will assume that no CO_2 is consumed by dissolution in brine.

6.4   *Incorporation of CO$_2$ in Biomass*

If significant microbial activity occurred in the WIPP during the 10,000 year regulatory time period, it is possible that organic carbon in CPR materials would be incorporated into biomass (cellular material) rather than "being oxidized to CO_2" (Brush and Roselle 2006). This process is relevant to the EEF calculation because incorporation of significant quantities of carbon into biomass could potentially affect the quantity of MgO that would be required to sequester microbially generated CO_2. However, Brush and Roselle (2006) state that "it would be difficult to predict defensibly how much C would be sequestered in biomass… Because of potential difficulties in calculating and defending the mass and ultimate fate of biomass in the WIPP, we cannot quantify this uncertainty."

Because the uncertainty in the quantity of organic carbon that might be sequestered in biomass cannot presently be quantified, this analysis will conservatively assume that no organic carbon in CPR materials will be incorporated into biomass. If it was possible to quantify this uncertainty and the uncertainty was included in calculation of the EEF, it would have the impact of increasing the mean EEF and increasing the standard deviation. The magnitudes of these changes are not known.

6.5   *Quantifying r*

The analysis shown in Section 6.1 makes three conservative assumptions:
1) 1 mole of CO_2 is generated for each mole of consumed organic carbon.
2) CO_2 is produced at the maximum CO_2 generation rate that is used in WIPP PA.
3) The half life for the conversion of hydromagnesite to magnesite is 273 years.

Even with these conservatisms, the analysis shows that uncarbonated magnesium will always remain in the repository after all of the CPR has been consumed if DOE emplaces an EF of 1.2. Due to the conservative nature of the calculations in Section 6.1, this analysis assumes that each mole of MgO will consume one mole of CO_2. Furthermore, this analysis will make the following assumptions:
1) CO_2 will not be consumed by Fe-base metals or their corrosion products, Pb-base metals or their corrosion products, or lime and portlandite in portland cements.
2) No CO_2 is consumed by dissolution in brine.
3) No organic carbon in CPR materials will be incorporated into biomass.

Thus, this analysis assigns a constant value of 1.0 to *r*.

7.0 Calculation of the MgO Effective Excess Factor

As indicated in Section 3.0, there are three primary sources of uncertainty included in the Effective Excess Factor calculation:
1) uncertainties in the quantities of CO_2 produced by microbial consumption of the CPR;
2) uncertainties in the amount MgO that is available to consume CO_2; and
3) uncertainties in the moles of CO_2 sequestered by each mole of available MgO.

Eq. 7-1 incorporates all of the quantified uncertainties that are included in the EEF calculation.

7-1
$$EEF = \frac{m \times M_{MgO}}{g \times M_C} \times r = \frac{\left(y_{SS} \times y_{RC} \times 0.999 - y_{L2B}\right) \times M_{MgO}}{\left(y_{yield} \times y_{CPR}\right) \times M_C} \times r$$

The term M_C is the total moles of organic carbon in the emplaced CPR mass, and M_{MgO} is the total moles of emplaced MgO. The variables g and m are random variables defined in Eqs. 4-10 and 5-8 and represent the uncertainty in the quantities of CO_2 produced and the uncertainty in the amount of MgO available for CO_2 consumption, respectively. The r term represents the moles of CO_2 consumed by each mole of emplaced MgO and is constant.

Table 3, Table 4, and Table 5 list all of the issues discussed in Sections 4.0, 5.0, and 6.0 that could potentially affect calculation of the EEF. These tables indicate in which sections the issues were discussed, how the issues are included in the EEF calculation, and means and standard deviations if the issues were quantified or how the issue could potentially impact the EEF calculation if the issue was not completely quantified.

Table 3 Issues Affecting CO_2 Production

Issue	Section	Inclusion in EEF as Random Variable (RV) or Assumption?	Mean (μ) and Std. Dev. (σ) if RV / Expected Impact if not RV
CPR Estimates	4.1	RV: y_{CPR}	$\mu_{CPR} = 1.00$, $\sigma_{CPR} = 3 \times 10^{-3}$
Effective CO_2 yield	4.2 and subsections of 4.2	RV: y_{yield}	$\mu_{yield} = 0.715$ moles CO_2 per mole of consumed organic carbon, $\sigma_{yield} = 0.0158$ moles CO_2 per mole of consumed organic carbon
Methanogenesis	4.2.2	Assume that methanogenesis does not occur.	Inclusion of methanogenesis would increase mean EEF and increase uncertainty.

Table 4 Issues Affecting the Percentage of MgO Available for CO_2 Sequestration

Issue	Section	Inclusion in EEF as Random Variable (RV) or Assumption?	Mean (μ) and Std. Dev. (σ) if RV / Expected Impact if not RV
Concentration of reactive constituents in MgO	5.1.1	RV: y_{RC}	$\mu_{RC} = 0.96$, $\sigma_{RC} = 0.02$
Carbonation of MgO prior to emplacement	5.1.2	Assume that 0.1% of MgO carbonates prior to emplacement.	Conservative assumption decreases the mean EEF.
Ability of periclase to react to completion	5.1.3	Assume that all periclase will react until all CO_2 is consumed.	Inclusion of this uncertainty in the EEF could decrease the mean and increase the uncertainty for the EEF. The expected magnitude of these changes is small.
Loss of MgO to brine	5.2.2	RV: y_{L2B}	$\mu_{L2B} = 0.008$, $\sigma_{L2B} = 0.019$
Rupturing of supersacks	5.2.1	Assume that all MgO supersacks rupture.	Certainty of this process results in no impact on EEF.
Amount of MgO in each room relative to the amount tracked by DOE	5.2.5	RV: y_{SS}	$\mu_{SS} = 1.00$, $\sigma_{SS} = 3.7 \times 10^{-4}$
Mixing processes	5.2.3	Assume that a well-mixed brine will be maintained.	Certainty of this process results in no impact on EEF.
Physical segregation of MgO from CO_2	5.2.4	No MgO is rendered unavailable for CO_2 consumption due to physical segregation.	Inclusion of this uncertainty in the EEF could decrease the mean and increase the uncertainty for the EEF. The expected magnitude of these changes is small.

Table 5 Issues Affecting the Moles of CO_2 Consumed by a Single Mole of Available MgO

Issue	Section	Inclusion in EEF as Random Variable (RV) or Assumption?	Mean (μ) and Std. Dev. (σ) if RV / Expected Impact if not RV
Hydromagnesite and magnesite formation	6.1 and 6.5	Assume that 1 mole of MgO will consume 1 mole of CO_2	The constant r = 1 mole of CO_2 consumed per mole of available MgO.
Consumption of CO_2 by materials other than MgO	6.2	Assume Fe-base metals or their corrosion products, Pb-base metals or their corrosion products, or lime and portlandite in portland cements do not consume CO_2	Inclusion of CO_2 consumption by these materials could increase the mean EEF and increase uncertainty.
Dissolution of CO_2 in WIPP brines	6.3	Assume CO_2 is not consumed by dissolution in brine.	Exclusion of this process results in no impact on EEF because of the extremely small quantities of CO_2 that could be consumed by this mechanism.
Incorporation of CO_2 in biomass	6.4	Assume no organic C is sequestered in biomass.	Inclusion of sequestration of organic C in biomass would increase the mean EEF and increase uncertainty.

7.1 *Calculated EEF Means and Uncertainties*

Using Eq. 7-1, the means, standard deviations, and relative uncertainties were calculated for the random variables g, m, and EEF (Table 6). The mean EEF (1.60) is 60% larger than the level required to maintain chemical conditions predicted in PA, and the standard deviation for EEF is 0.0819. (The calculations for the results presented in this section and the associated statistical methods used in these calculations are detailed in Appendix C.)

Table 6 Means and Uncertainties for the Random Variables g, m, and EEF

Variable	Mean	Standard Deviation	Relative Uncertainty
g	$\mu_g = 0.715$	$\sigma_g = 0.0159$	$\dfrac{\sigma_g}{\left|\mu_g\right|} = 0.0223$
m	$\mu_m = 0.951$	$\sigma_m = 0.0276$	$\dfrac{\sigma_m}{\left|\mu_m\right|} = 0.0290$
EEF	$\mu_{EEF} = 1.60$	$\sigma_{EEF} = 0.0819$	$\dfrac{\sigma_{EEF}}{\left|\mu_{EEF}\right|} = 0.0513$

The EEF distribution is assigned a mean of 1.60 and standard deviation of 0.0819. The Central Limit Theorem of Statistics shows that products and quotients of random variables tend to converge to lognormal distributions, which are positively skewed (Aitchison and Brown 1981, Morgan and Henrion 1992). This analysis assumes that the EEF is lognormally distributed since the EEF calculation involves both products and quotients of random variables. The geometric mean (GM) and geometric standard deviation (GSD) for EEF are calculated to be 1.59 and 1.05, respectively. Under the assumption of lognormality, there is a 3×10^{-5} probability that the EEF will be less than 1.30 (Table 7), which is 30 % higher than the minimum EEF required to maintain chemical conditions assumed in PA. Furthermore, there is only a 10^{-19} probability that the EEF will be less than 1.01. There is some uncertainty as to whether the EEF probability distribution is lognormal, normal, or some other probability distribution. However, because the GSD is close to 1.0, this distribution is nearly symmetric. Therefore, assuming that the distribution is normal or some similar distribution would have little impact in the conclusions. Thus, there is little likelihood that an EF equal to 1.2 will be insufficient to maintain chemical conditions.

Table 7 Cumulative Probabilities for Several EEF Values

Y	$P\left(EEF < Y\right)$
1.52	0.1587
1.44	0.0228
1.37	0.0013
1.30	3×10^{-5}
1.23	3×10^{-7}
1.17	1×10^{-9}
1.11	1×10^{-12}
1.06	6×10^{-16}
1.01	1×10^{-19}

8.0 Summary and Conclusions

The EPA currently requires the DOE to emplace 1.67 moles of MgO for every mole of organic carbon in emplaced CPR. The EPA has stated that they require this "relatively high excess amount" since "the extra MgO would overwhelm any perceived uncertainties that the chemical reactions would take place as expected" (Gitlin 2006). Thus, when the DOE requested that the MgO excess factor be lowered from 1.67 to 1.2, the EPA required that the DOE address "the uncertainties related to MgO effectiveness, the size of the uncertainties, and the potential impact of the uncertainties on long-term performance" (Gitlin 2006). To address this request, SNL has conducted an analysis of these uncertainties.

This analysis introduces the concept of the MgO "Effective Excess Factor," a quantity that incorporates uncertainties into the current definition of the MgO excess factor. The uncertainties included in the EEF calculation are grouped into three categories:
1) uncertainties in the quantities of carbon dioxide (CO_2) produced by microbial consumption of the CPR;
2) uncertainties in the amount MgO that is available to react with CO_2; and
3) uncertainties in the moles of CO_2 sequestered per mole of MgO that is available to consume CO_2.

This analysis includes the conservative assumption that microbes will consume all of the organic carbon in the CPR materials that are emplaced in the repository. While this analysis has not attempted to quantify the percentages of CPR that might be consumed or the probabilities associated with these percentages, inclusion of this uncertainty in calculation of the EEF has the potential to significantly increase the mean EEF (Appendix A). The potential impact on the EEF of this assumption and other uncertainties that cannot presently be quantified are qualitatively analyzed. The remaining uncertainties that were quantified are represented in the EEF calculation with random variables.

Since the EEF considers the uncertainties affecting MgO effectiveness, it is necessary only for the EEF to be greater than 1 to maintain chemical conditions as assumed in WIPP PA. Using standard techniques from measurement theory, the quantified uncertainties of the individual components were propagated to calculate the mean and uncertainty for the EEF. If 1.2 moles of MgO are emplaced for every mole of organic carbon in emplaced CPR, the mean EEF is 1.60 and the standard deviation (uncertainty) is less than 0.0819.

Under the assumption that the EEF is lognormally distributed with mean equal to 1.60 and standard deviation equal to 0.0819, there is a 3×10^{-5} probability that the EEF will be less than 1.30, 30% higher than the minimum EEF required to maintain chemical conditions assumed in PA. Furthermore, there is only a 10^{-19} probability that the EEF will be less than 1.01. Because the magnitude of this probability is so small and because many conservatisms have been incorporated into the calculation of the EEF, this analysis concludes that emplacing 1.2 moles of MgO for every mole of organic carbon in the emplaced CPR is more than sufficient to maintain chemical conditions as assumed in WIPP PA.

9.0 References

Aitchison, J., and J. A. C. Brown. 1981. The Lognormal Distribution. Cambridge University Press, New York, NY. pp. 22-3.

Brooks, R., L.M. Clark, and E.F. Thurston. 1950. "Calcium Carbonate and its Hydrates." *Philosophical Transactions of the Royal Society of London, Series A*. Vol. 243, 145-168.

Brush, L.H. 1995. Systems Prioritization Method - Iteration 2 Baseline Position Paper: Gas Generation in the Waste Isolation Pilot Plant. Sandia National Laboratories. Albuquerque, NM. ERMS 228740.

Brush, L.H. 2004. Implications of New (Post-CCA) Information for the Probability of Significant Microbial Activity in the WIPP. Sandia National Laboratories. Carlsbad, NM. ERMS 536205.

Brush, L. H., and G. T. Roselle. 2006. Geochemical Information for Calculation of the MgO Excess Factor. Memo to Eric D. Vugrin, November 17, 2006. Sandia National Laboratories. Carlsbad, NM.

Brush, L. H., Y. Xiong, J. W. Garner, A. E. Ismail, and G. T. Roselle. 2006. Consumption of Carbon Dioxide by Precipitation of Carbonate Minerals Resulting from Dissolution of Sulfate Minerals in the Salado Formation in Response to Microbial Sulfate Reduction in the WIPP. Sandia National Laboratories. Carlsbad, NM.

Clayton, D. J. and M. B. Nemer. 2006. Normalized Moles of Castile Sulfate Entering the Repository and Fraction of MgO Lost Due to Brine Flow Out of the Repository. Memo to Eric D. Vugrin, October 9th, 2006. Sandia National Laboratories. Carlsbad, NM. ERMS 544385.

Cotsworth, E. 2004. Untitled letter with enclosure to R.P. Detweiler with first set of CRA comments, May 20, 2004. Washington, DC: U.S. Environmental Protection Agency Office of Air and Radiation. ERMS 535554.

Cotsworth, E. 2005. EPA Letter on Conducting the Performance Assessment Baseline Change (PABC) Verification Test. U.S. EPA, Office of Radiation and Indoor Air. Washington, D.C. ERMS 538858.

Deal, D. E., R. J. Abitz, D. S. Belski, J. B. Case, M. E. Crawley, C. A. Givens, P. P. J. Lipponer, J. Myers, D. W. Powers, and M. A. Valdiva. 1995. Brine Sampling and Evaluation Program 1992-1993 Report and Summary of BSEP Data Since 1982. Contractor Report DOE-WIPP 94-011, U.S. Department of Energy WIPP Project Office. Carlsbad, NM.

Deng, H., S. Johnsen, G. Roselle, and M. Nemer. 2006a. Preliminary Analysis of Martin Marietta MagChem 10 WTS-60 MgO. Sandia National Laboratories. Carlsbad, NM. ERMS 544712.

Deng, H., M.B. Nemer, and Y. Xiong. 2006b. Experimental Study of MgO Reaction Pathways and Kinetics, Rev. 0. TP 06-03, Rev. 0, June 6, 2006. Sandia National Laboratories. Carlsbad, NM. ERMS 543633.

DOE. 1983a. Results of Site Validation Experiments, Waste Isolation Pilot Plant (WIPP) Project, Southeastern New Mexico. Vol. I. Executive Summary, Text, and Supporting Documents 1 through 4. TME-3177, Vol. I, U.S. Department of Energy Waste Isolation Pilot Plant, Albuquerque, NM.

DOE. 1983b. Results of Site Validation Experiments, Waste Isolation Pilot Plant (WIPP) Project, Southeastern New Mexico. Vol. II. Supporting Documents 5 through 14. TME-3177, Vol. II, U.S. Department of Energy Waste Isolation Pilot Plant, Albuquerque, NM.

DOE. 1996. Title 40 CFR Part 191 Compliance Certification Application for the Waste Isolation Pilot. DOE/CAO-1996-2184, U.S. Department of Energy Waste Isolation Pilot Plant, Carlsbad Area Office, Carlsbad, NM.

DOE. 1997. DOE Response to Comments to EPA December 19, 1996 letter, EPA docket A-93-02 Item II-I-10, EPA Comment Enclosure 2, Page 3, 194.23(a)(3)(i) February 1997.

DOE. 2000. Proposal for Elimination of MgO Mini-sacks. U. S. Department of Energy Carlsbad Field Office, Carlsbad, NM. ERMS 543262.

DOE. 2004a. Title 40 CFR Part 191 Compliance Recertification Application for the Waste Isolation Pilot Plant, Vol. 1-8. DOE/WIPP 2004-3231. U.S. Department of Energy Carlsbad Field Office. Carlsbad, NM.

DOE. 2004b. DOE's 6th Response Submittal to Comments from EPA's 2nd Request for Additional Information December 2004.

DOE. 2005. Letter from Ines Tray, Acting Manager of the Carlsbad Field Office to Bonnie Gitlin, Acting Director of EPA Radiation Protection Division, Plans for Emplacement of Additional MgO, March 8, 2005.

EPA. 2004a. Review of Effects of Supercompacted Waste and Heterogeneous Waste Emplacement on WIPP Repository Performance. Washington D.C.

EPA. 2004b. Letter from Elizabeth Cotsworth, EPA Director of Radiation and Indoor Air to Paul Detwiler, CBFO Acting Manager requesting additional information for a completeness determination, ERMS 536771.

Gal, J. Y., J. C. Bollinger, H. Tolosa, and N. Gache. 1996. "Calcium Carbonate Solubility: A Reappraisal of Scale Formation and Inhibition," *Talanta*. Vol. 43, no. 9, 1497-1509.

Gillow, J. B., and A. J. Francis. 2003. Microbia; Gas Generation Under Expected Waste Isolation Pilot Plant Conditions: Draft Final Report, Rev. 0, October 6, 2003. Brookhaven National Laboratory. Upton, NY. ERMS 532877.

Gitlin, B. C. 2006. Letter to D. C. Moody Concerning the DOE's Request to Reduce the MgO Excess Factor from 1.67 to 1.2, dated April 28, 2006.

Hailey, S. M. 1994. A Comparison of Real-Time Radiography Results and Visual Characterization Results with Emphasis on WIPP WAC and TRAMPAC Compliance Issues. Idaho National Laboratory. Idaho Falls, ID.

Hansen, C. W., L. H. Brush, M. B. Gross, F. D. Hansen, B.-Y. Park, J. S. Stein, and T. W. Thompson. 2004. Effects of Supercompacted Waste and Heterogeneous Waste Emplacement on Repository Performance, Revision 2. Sandia National Laboratories. Carlsbad, NM. ERMS 533551.

Hansen, F. D. 2005. Magnesium Super Sack Rupture under WIPP Conditions. Memo to D. Kessel, dated May 11, 2005. Sandia National Laboratories. Carlsbad, NM. ERMS 539724.

Kanney, J. F., A. C. Snider, T. W. Thompson, and L. H. Brush. 2004. Effect of Naturally Occurring Sulfate on the MgO safety Factor in the Presence of Supercompacted Waste and Heterogenous Waste Emplacement. Sandia National Laboratories. Carlsbad, NM. ERMS 534150.

Kanney, J. F. and E. D. Vugrin. 2006. Updated Analysis of Characteristic Time and Length Scales for Mixing Processes in the WIPP Repository to Reflect the CRA-2004 PABC Technical Baseline and the Impact of Supercompacted Mixed Waste and Heterogeneous Waste Emplacement. Sandia National Laboratories. Carlsbad, NM. ERMS 544248.

Katz, A. 1973. "The Interaction of Magnesium with Calcite during Crystal Growth at 25–90 °C and One Atmosphere," *Geochimica et Cosmochimica Acta*. Vol. 37, no. 6, 1563-1578.

Kirchner, T. B. and E. D. Vugrin. 2006. Uncertainty in Cellulose, Plastic, and Rubber Measurements for the Waste Isolation Pilot Plant Inventory. Sandia National Laboratories, Carlsbad, NM. ERMS 543848.

Knight, W. 2006. Tables of the Normal Distribution. Sandia National Laboratories, Carlsbad, NM. ERMS 544302.

Marcinowski, F. 2001. Environmental Protection Agency's (EPA's) Approval for the Elimination of Magnesium Oxide (MgO) Mini-sacks from WIPP. Sandia National Laboratories, Carlsbad, NM. ERMS 519362.

Mood, A. M., F. A. Graybill and D. C. Boes. 1974. Introduction to the Theory of Statistics. McGraw-Hill, New York, NY.

Moody, D. C. 2006. Letter to E. A. Cotsworth Requesting a Reduction in the MgO Excess Factor from 1.67 to 1.2, dated April 10, 2006. ERMS 543262.

Morgan, M. G., and M. Henrion. 1992. Uncertainty: A Guide to Dealing with Uncertainty in Quantitative Risk and Policy Analysis. Cambridge University Press, New York, NY. pp. 186-7.

Nemer, M. B. and J. S. Stein 2005. Analysis Package for BRAGFLO, 2004 Compliance Recertification Application Performance Assessment Baseline Calculation. Sandia National Laboratories, Carlsbad, NM. ERMS 540527.

Popielak, R. S., R. L. Beauheim, S. R. Black, W. E. Coons, C. T. Ellingson, and R. L. Olsen. 1983. Brine Reservoirs in the Castile Formation, Waste Isolation Pilot Plant (WIPP) Project, Southeastern New Mexico. TME-3153, U.S. Department of Energy Waste Isolation Pilot Plant, Albuquerque, NM.

Snider, A. C. 2003a. Calculation of MgO Safety Factors for the WIPP Compliance Recertification Application and for Evaluating Assumptions of Homogeneity in WIPP PA. Analysis report, September 11, 2003. Sandia National Laboratories. Carlsbad, NM. ERMS 531508.

Snider, A.C. 2003b. "Verification of the Definition of Generic Weep Brine and the Development of a Recipe for This Brine." Analysis report, April 8, 2003. Carlsbad, NM: Sandia National Laboratories. ERMS 527505.

Taylor, J. R. 1982. An Introduction to Error Analysis: The Study of Uncertainties in Physical Measurements. University Science Books, Mill Valley, CA.

Vugrin, E. D. 2006. Total Number of MgO Supersacks per Room in Panels 1, 2, and 3 as of August 17, 2006. Carlsbad, NM. Sandia National Laboratories. ERMS 544234.

Wall, N.A. 2005. "Preliminary Results for the Evaluation of Potential New MgO." Sandia National Laboratories. Carlsbad, NM. ERMS 538514.

Wang, Y. and L.H. Brush. 1996. "Estimates of Gas-Generation Parameters for the Long-Term WIPP Performance Assessment." Memorandum to M.S. Tierney, January 26, 1996. Sandia National Laboratories. Albuquerque, NM. ERMS 231943.

Wang, Y. 2000. Effectiveness of Mixing Processes in the Waste Isolation Pilot Plant Repository. Technical Memorandum. Sandia National Laboratories, Carlsbad, NM. ERMS 519362.

Westin, K., and A.C. Rasmuson. 2005. "Crystal Growth of Aragonite and Calcite in Presence of Citric Acid, DTPA, EDTA and Pyromellitic Acid," *Journal of Colloid and Interface Science*. Vol. 282, no. 2, 359-369.

Wolery, T.J., and S.A. Daveler. 1992. EQ6, A Computer Program for Reaction-Path Modeling of Aqueous Geochemical Systems: Theoretical Manual, User's Guide, and

Related Documentation (Version 7.0). UCRL-MA-110662 PT IV. Livermore, CA: Lawrence Livermore National Laboratory.

WTS. 2005. Specifications for Repackaged Backfill, Waste Isolation Pilot Plant Procedure D-0101, Revision 7, May 2005.

WTS. 2006. CH Waste Processing, Technical Procedure WP05-WH1011, Revision 23, January 2006.

10.0 Appendix A

The calculation of the EEF includes the conservative assumption that all of the organic carbon in the emplaced CPR materials will be consumed by microbes. This assumption affects the quantity of CO_2 that can be produced by microbial respiration and, hence, impacts the EEF calculation.

Even though this analysis conservatively assumes that all of the organic carbon will be consumed, it should be noted that, in fact, there are several uncertainties associated with this assumption. In keeping with the EPA's direction that "DOE needs to address the uncertainties related to MgO effectiveness, the size of the uncertainties, and the potential impact of the uncertainties on long-term performance" (Gitlin 2006), the uncertainties associated with this assumption are qualitatively discussed in this appendix.

Several factors affect the quantity of organic carbon in CPR materials that could be consumed by microbes. Brush (1995) described seven issues:
1) Whether microbes will be present in the repository when it is filled and sealed;
2) Whether the emplaced waste and other contents of the repository will be sterilized;
3) Whether microbes will survive for a significant fraction of the 10,000 year regulatory time frame;
4) Whether sufficient water will be present for significant microbial respiration to take place;
5) Whether sufficient quantities of biodegradable substrates will be present for significant microbial respiration to take place;
6) Whether sufficient electron acceptors will be present and available for significant microbial respiration to take place; and
7) Whether enough nutrients, especially N and P, will be present and available for significant microbial respiration to take place.

These issues, identified in Brush (1995) and updated in Brush (2004), are summarized herein.

10.1 *Presence of Microbes in the Repository*

Brush (1995) concluded "halophilic microorganisms capable of carrying out [potentially significant] respiratory pathways … probably exist throughout the WIPP underground workings." DOE (2004a, Appendix Barriers) further notes that the results of the long-term Brookhaven National Laboratory (BNL) study of microbial gas generation (Gillow and Francis 2003) "have confirmed that viable halophilic fermenters and methanogens capable of metabolizing cellulosic materials under expected near-field conditions are present in the WIPP underground workings." Thus, Brush (2004) concluded that halophilic microbes are expected to be present and that this issue was not a significant source of uncertainty.

10.2 *Sterilization of the Waste and Other Repository Contents*

Brush (1995) states that sterilization of the waste to preclude microbial activity is infeasible. However, Brush (2004) states that MgO and compounds derived from MgO have been observed to possess inhibitory or even biocidal properties. Generally, biocides are required to be in contact with microbes to ensure that the biocide is effective. The large volume of waste in rooms in the repository would make it difficult to ensure contact between the MgO and microbes, so it is unlikely that the presence of MgO would preclude all microbial activity (Appendix Barriers, DOE 2004a). However, it is possible that the MgO could reduce the rate of microbial gas generation in the WIPP (Appendix Barriers, DOE 2004a), and a reduction in microbial gas generation rates could potentially limit the amount of organic carbon in CPR materials that could be consumed.

Inhibition of microbial activity by MgO has not been quantified in repository-specific laboratory experiments simulating expected WIPP conditions. Because of the uncertainties associated with the possible inhibition or reduction of microbial activity, this issue is conservatively excluded from the uncertainty analysis.

10.3 *Survivability of Microbes*

As discussed in Section 10.1, there is a high probability that microbes will be present when the repository is closed. However, after the shafts and surrounding boreholes are sealed, the contents of the repository will be isolated from the surface environment until a potential human intrusion. Thus, the survivability of microbes for a significant period of time during the 10,000 year regulatory time period is a large and important source of uncertainty.

As discussed in Brush (2004), the rates of microbial activity and microbial gas production in the long-term BNL study of microbial gas generation by Gillow and Francis (2003) were "relatively high initially, but soon decreased significantly, and have quite possibly decreased to zero" (Brush 2004). Brush (2004) further states that because the gas production has ceased or nearly ceased after less than 0.1% of the 10,000 year regulatory time period, the results of Gillow and Francis (2003) decrease the certainty that microbes will survive long enough to affect repository performance.

Brush (2004) also notes that the presence of MgO may decrease the survivability of microbes through two separate mechanisms. First, as described in Section 10.2, the MgO may possess biocidal or inhibitory properties that affect microbes. Secondly, hydration of MgO will maintain dry conditions for a potentially significant period of time, thereby decreasing the probability of survival of viable microbes.

10.4 *Presence of Sufficient Quantities of Water*

Hydration of MgO will maintain dry conditions in the repository for a potentially significant period of time, thus limiting the quantities of water available to microbes for a potentially significant period of time (Brush 2004). This length of time has not been precisely quantified, but "this period could be long enough - and the activity of water during this period could be low

enough - to decrease the probability of survival of microbes" (Brush 2004). Hence, the amount of organic carbon in CPR materials that is consumed by microbial activity could be affected by MgO hydration and a lack of available water.

10.5 *Presence of Sufficient Quantities of Biodegradable Substrates*

As discussed in Section 10.3, the rates of microbial activity and gas production in the BNL study of microbial gas generation were initially relatively high before decreasing significantly, and quite possibly ceasing altogether (Gillow and Francis 2003). Brush (2004) reported that less than 5% of cellulosic materials were consumed before gas production ceased or nearly ceased, and there was very limited gas production from the irradiated plastic and rubber materials. Though these results are from a study that was carried out for less than 0.1% of the 10,000 year regulatory time period, they add to the uncertainty that all of the CPR materials will be consumed. DOE plans to further investigate this issue in the future.

10.6 *Presence of Sufficient Electron Acceptors*

Cotsworth (2004) stated,

> "*In addition, sulfate present in brine and in minerals in the Salado Formation surrounding the repository are likely to be available for reaction, so sufficient electron acceptors may be expected to be present.*"

If sulfate from the brine and minerals in the Salado Formation was readily available to microbes in the repository, this source alone would be a sufficient source of electron acceptors. Kanney et al. (2004) conducted an analysis that conservatively bounds the quantities of sulfate that could enter the repository via diffusion and advection, but amongst other issues, the EPA commented that roof collapse could bring sulfate-bearing minerals[8] into direct contact with brines in the repository (EPA 2004a). Thus, there is considerable uncertainty in the amount of sulfate that would be present in the repository.

However, even if the amount of sulfate was limited, microbial consumption of CPR materials is expected to proceed via methanogenesis. Hence, the possibility of the presence of sufficient electron acceptors cannot be ruled out presently.

10.7 *Presence of Sufficient Nutrients*

Brush (2004) states that microbes require a variety of nutrients, including C, O, N, H, P, S, K, Na, Ca, Mg, Cl, Fe, Mn, Zn, Mo, Cu, and Co. Many of these nutrients are found in WIPP brines and waste materials. However, Brush (2004) indicates that "it is unclear whether nutrients would actually be available to microbes. For example, precipitation of PO_4^{3-} by highly insoluble phases

---

[8] It should be noted that the sulfate-bearing minerals found in the disturbed rock zone also contain significant quantities of calcium. The presence of calcium is significant because the calcium has the potential to react with CO_2 and precipitate $CaCO_3$-bearing minerals, thus sequestering CO_2. This process is discussed in Section 4.2.1.1 and Brush et al. (2006).

such as apatite ($Ca_5(PO_4)_3(OH,F,Cl)$) could effectively sequester this nutrient, especially if apatite contains appreciable concentrations of inhibitory, toxic, or radiotoxic heavy metals such as the actinides in TRU [transuranic] waste." Hence, it is uncertain whether microbes will have sufficient nutrients for significant microbial activity.

10.8 *Impact of the Uncertainties on the MgO Excess Factor*

None of the uncertainties discussed in Sections 10.1-10.7 are included in this analysis because calculation of the MgO excess factor and the MgO EEF includes the conservative assumption that all of the organic carbon in CPR materials can and will be consumed by microbial activity. If these uncertainties could be quantified and were included in the EEF calculations, they would have the effect of reducing the expected amount of CO_2 that could be produced and of increasing the uncertainty. Consequently, the expected impact of including these uncertainties is an increase in the mean EEF and an increase in the EEF's standard deviation. The magnitude of these increases is not presently known.

11.0 Appendix B

For the CRA-2004, Snider (2003a) estimated that if all of the CPR materials in the inventory were consumed sequentially by denitrification, sulfate reduction, and methanogenesis, 4.72 mole % of the organic carbon in CPR materials will be consumed by denitrification and 0.82 mole % by SO_4^{2-} reduction. This appendix updates this calculation for the CRA-2004 PABC inventory.

The CRA-2004 PABC calculations assumed that 1.10×10^9 moles of organic carbon were present in the emplaced CPR materials (Nemer and Stein 2005), and Table 8 lists the masses of nitrates and sulfates in the emplaced waste materials for the CRA-2004 PABC calculations. When all of the organic carbon in the emplaced CPR materials is consumed, 4.89 mole % of the organic carbon will be consumed by denitrification (Eq. 11-1). Additionally, up to 0.84 mole % of the organic carbon can be consumed by sulfate reduction using sulfate contained in the waste materials (Eq. 11-2). (The ratio of moles of carbon consumed per mole of nitrate and sulfate are determined by Eqs. 4-3 and 4-4.) The percentages of carbon consumed by each pathway differs slightly from Snider's (2003) results because the quantities of nitrates, sulfates, and CPR materials were revised and updated for the CRA-2004 PABC calculations.

Table 8 Initial Quantities of Sulfates and Nitrates in the Emplaced Waste (Nemer and Stein 2005)

Material	Property	Description	CRA-2004 PABC Value
NITRATE	QINIT	Initial quantity of NO_3^- in waste (moles)	4.31×10^7
SULFATE	QINIT	Initial quantity of SO_4^{2-} in waste (moles)	4.61×10^6

$$11\text{-}1 \qquad \frac{4.31 \times 10^7 \text{ moles NO}_3^- \times \dfrac{6 \text{ moles C consumed in denitrification}}{4.8 \text{ moles NO}_3^-}}{1.10 \times 10^9 \text{ moles C in CPR materials}} = 0.0489$$

$$11\text{-}2 \qquad \frac{4.61 \times 10^6 \text{ moles SO}_4^{2-} \times \dfrac{6 \text{ moles C consumed in SO}_4^{2-} \text{ reduction}}{3 \text{ moles SO}_4^{2-}}}{1.10 \times 10^9 \text{ moles C in CPR materials}} = 0.0084$$

12.0 Appendix C

As indicated in Eq. 7-1, the EEF is a random variable since it is a function of random variables. The following sections detail how to calculate the mean and uncertainty (standard deviation) for the random variables g, m, and EEF.

12.1 *Background*

Before calculating the mean and uncertainties associated with the EEF, it is necessary to state the theorems required for these calculations. Theorem 1 can be used to calculate the mean of a random variable that is the function of two independent random variables, X and Y (Mood et al. 1974):

> **Theorem 1:** *Let X and Y be independent random variables with means μ_X and μ_Y, respectively. If Z=X± Y, W = X ×Y , and V=cX where c is a constant, then their respective means are $\mu_Z = \mu_X \pm \mu_Y$, $\mu_W = \mu_X \times \mu_Y$, and $\mu_V = c\mu_X$.*

Mood et al. (1974) state that there are no simple formulas for calculating the mean of the quotient of two random variables. The following theorem from Mood et al. (1974) is useful for approximating the mean:

> **Theorem 2:** *Let X and Y be random variables with respective means μ_X and μ_Y. If Z=X/Y, then*

12-1
$$\mu_Z \approx \frac{\mu_X}{\mu_Y} - \frac{1}{\mu_Y^2}\text{cov}[X,Y] + \frac{\mu_X}{\mu_Y^3}\text{var}[Y.]$$

The following two theorems from Taylor (1982) are used to calculate the uncertainties for g and m:

> **Theorem 3:** *Suppose X and Y are measured with uncertainties σ_X and σ_Y, and the measured values are used to compute Z=X± Y. If the uncertainties in X and Y are known to be independent and random, then the uncertainty in Z, σ_Z, is*

12-2
$$\sigma_Z = \sqrt{\left(\sigma_X\right)^2 + \left(\sigma_Y\right)^2}.$$

> *In any case,*

12-3
$$\sigma_Z \le \sigma_X + \sigma_Y.$$

> **Theorem 4:** *Suppose X and Y are measured with uncertainties σ_X and σ_Y, and the measured values are used to compute $Z = X \times Y$ and $W = X/Y$. If the uncertainties in X and Y are known to be independent and random, then the fractional uncertainties in Z and W, $\dfrac{\sigma_Z}{|Z|}$ and $\dfrac{\sigma_W}{|W|}$, are*

12-4
$$\frac{\sigma_Z}{|Z|} = \frac{\sigma_W}{|W|} = \sqrt{\left(\frac{\sigma_X}{|X|}\right)^2 + \left(\frac{\sigma_Y}{|Y|}\right)^2}.$$

In any case,

12-5
$$\frac{\sigma_Z}{|Z|} \leq \frac{\sigma_X}{|X|} + \frac{\sigma_Y}{|Y|}$$

and

12-6
$$\frac{\sigma_W}{|W|} \leq \frac{\sigma_X}{|X|} + \frac{\sigma_Y}{|Y|}.$$

12.2 Calculating the Random Variables g and m

Recall from Eqs. 4-10 and 5-8 that the random variables g and m in the EEF calculation are defined as follows:

12-7
$$g = y_{yield} \times y_{CPR}$$

12-8
$$m = y_{SS} \times y_{RC} \times 0.999 - y_{L2B}$$

Before calculating the means and standard deviations of g and m, the independence of the random variables y_{yield}, y_{CPR}, y_{SS}, y_{RC}, and y_{L2B} must be examined. Since the estimation techniques that are used to calculate quantities of CPR that are emplaced in the repository are independent from the microbial respiration pathways that consume the organic carbon in the emplaced CPR materials, it is reasonable to assume that the random variables y_{yield} and y_{CPR} are independent. Additionally, the mass of an MgO supersack is independent of the percentage of reactive constituents of the materials in that supersack, so the random variables y_{SS} and y_{RC} are independent. The amount of MgO lost to brine outflow depends on the volumes of brine that leave the waste areas and the quantities of MgO dissolved in that brine. With the amounts of MgO that are expected to be emplaced in the repository, the quantities of MgO dissolved in brine will be independent of the mass of the supersacks and the percentage of reactive constituents in the emplaced MgO. The same is true for the amount of brine outflow. Hence, this analysis assumes that the variables y_{SS}, y_{RC}, and y_{L2B} are independent, and Theorems 1-4 can be used to calculate the means and standard deviations of the random variables g and m.

Application of Theorem 1 to Eqs. 12-7 and 12-8 results in a mean g value of 0.715 (μ_g=0.715) and a mean m value of 0.951 (μ_m =0.951) (Eqs. 12-9 and 12-10)[9].

12-9
$$\mu_g = \mu_{yield} \times \mu_{CPR}$$
$$= 0.715 \times 1.0 = 0.715$$

---

[9] Numerical values reported in Sections 12.2, 12.3, and 12.4 have been calculated in a spreadsheet and were then rounded for this document.

12-10
$$\mu_m = \mu_{SS} \times \mu_{RC} \times 0.999 - \mu_{L2B}$$
$$= 1.0 \times 0.96 \times 0.999 - 0.008 = 0.951$$

Furthermore, the fractional uncertainty in g, $\dfrac{\sigma_g}{|g|}$, is 0.0223 and is calculated by applying

Theorem 4 to Eq. 12-7. This calculation is shown in Eq. 12-11.

12-11
$$\frac{\sigma_g}{|\mu_g|} = \sqrt{\left(\frac{\sigma_{CPR}}{|\mu_{CPR}|}\right)^2 + \left(\frac{\sigma_{yield}}{|\mu_{yield}|}\right)^2}$$
$$= \sqrt{\left(\frac{0.003}{1.0}\right)^2 + \left(\frac{0.0158}{0.715}\right)^2}$$
$$= 0.0223$$

Eq. 12-12 indicates how to calculate the relative uncertainty in m using Theorem 3.

12-12
$$\frac{\sigma_m}{|\mu_m|} = \frac{\sqrt{(0.999 \times \sigma_{SS \times RC})^2 + (\sigma_{L2B})^2}}{|\mu_m|}$$

The term $\sigma_{SS \times RC}$ in Eq. 12-12 represents the uncertainty in the random variable $(y_{SS} \times y_{RC})$ and is calculated to be 0.02 (Eq. 12-13).

12-13
$$\sigma_{SS \times RC} = |\mu_{SS \times RC}| \times \sqrt{\left(\frac{\sigma_{SS}}{|\mu_{SS}|}\right)^2 + \left(\frac{\sigma_{RC}}{|\mu_{RC}|}\right)^2}$$
$$= 0.96 \times \sqrt{\left(\frac{3.7 \times 10^{-4}}{1.00}\right)^2 + \left(\frac{0.02}{0.96}\right)^2}$$
$$= 0.02$$

Consequently, the relative uncertainty in m is 0.0290 (Eq. 12-14).

12-14
$$\frac{\sigma_m}{|\mu_m|} = \frac{\sqrt{(0.999 \times 0.02)^2 + (0.019)^2}}{0.951} = 0.0290.$$

12.3 *EEF Calculation*

Before proceeding with the EEF calculation, it is necessary to assess if the random variables m and g are independent. A potential correlation between the two random variables y_{L2B} and y_{yield} may exist. As the number of E1 intrusions (intrusions that intersect a Castile brine pocket) increases, the quantity of brine that comes into and out of the repository increases, and thus, the amount of MgO dissolved in brine that leaves the repository could increase. Similarly, the amount of sulfate from the Castile brine pocket that enters the waste areas increases, resulting in a higher effective CO_2 yield per mole of consumed carbon. However, the number of E2

intrusions (intrusions that do not intersect a Castile brine pocket) impacts the loss of MgO to brine outflow but not the CO_2 yield. Thus, it is possible that the variables y_{L2B} and y_{yield}, and consequently m and g, are correlated, but the magnitude of the correlation is unknown.

If it is assumed that 1.2 moles of MgO are emplaced for every mole of organic carbon in the emplaced CPR, i.e. $M_{MgO} = (1.2)M_C$ in Eq. 7-1, then

12-15
$$EEF = \frac{m \times 1.2}{g}.$$

(Since r is equal to a constant value of 1.0 and will not affect any further calculations, it will not be explicitly shown in the remaining calculations). The mean EEF, μ_{EEF}, is calculated using Theorem 2 with the following equation:

12-16
$$\mu_{EEF} = 1.2 \left(\frac{\mu_m}{\mu_g} - \frac{\rho \sigma_m \sigma_g}{\mu_g^2} + \frac{\mu_m \sigma_g^2}{\mu_g^3} \right)$$
$$= 1.60 - (.001)\rho$$

The term ρ is the correlation coefficient for m and g. Because ρ is bounded between -1 and 1, the magnitude of the possible correlation does not significantly impact μ_{EEF}, and, thus, μ_{EEF} is approximately 1.60 regardless of the size of the correlation.

Because of the possible correlation between the random variables m and g, it is not appropriate to calculate the fractional uncertainty in EEF using Eq. 12-4 in Theorem 4. However, an upper bound on the fractional uncertainty can be determined using Eq. 12-6. Using this method, the fractional uncertainty in EEF, $\frac{\sigma_{EEF}}{|\mu_{EEF}|}$, is less than 0.0513 (Eq. 12-17), and the uncertainty σ_{EEF} is less than 0.0819 (Eq. 12-18).

12-17
$$\frac{\sigma_{EEF}}{|\mu_{EEF}|} \leq \frac{\sigma_m}{|\mu_m|} + \frac{\sigma_g}{|\mu_g|} = 0.0290 + 0.0223 = 0.0513$$

12-18
$$\sigma_{EEF} = \frac{\sigma_{EEF}}{|\mu_{EEF}|} \times |\mu_{EEF}| \leq 0.0513 \times 1.60 = 0.0819 .$$

12.4 *Calculation of EEF Associated Probabilities*

To assess the likelihood that maintaining an MgO EF of 1.2 is sufficient to "overwhelm the uncertainties" considered in the EEF, this analysis assumes that the random variable EEF is lognormally distributed with (arithmetic) mean μ_{EEF} equal to 1.60 and (arithmetic) standard deviation σ_{EEF} equal to 0.0819. The geometric mean (GM_{EEF}) and geometric standard deviation (GSD_{EEF}) are equal to 1.59 and 1.05, respectively (Eqs. 12-19 and 12-20). The Central Limit Theorem of Statistics shows that products and quotients of random variables tend to converge to lognormal distributions (Aitchison and Brown 1981, Morgan and Henrion 1992). Thus, this analysis assumes that the EEF is lognormally distributed since the EEF calculation involves both products and quotients of random variables.

12-19
$$GM_{EEF} = \exp\left(\ln(\mu_{EEF}) - \frac{1}{2}\ln\left(\frac{\sigma_{EEF}^2}{\mu_{EEF}^2} + 1 \right) \right) = 1.59$$

12-20
$$GSD_{EEF} = \exp\left(\sqrt{\ln\left(\frac{\sigma_{EEF}^2}{\mu_{EEF}^2} + 1 \right)} \right) = 1.05$$

Since

12-21
$$P(\ln(EEF) < \ln(y)) = P(EEF < y), \quad y > 0,$$

it is useful to consider the random variable $Z = \ln(EEF)$, which is normally distributed with mean equal to 0.467 ($\mu_Z = \ln(GM_{EEF})$) and standard deviation equal to 0.0513 ($\sigma_Z = \ln(GSD_{EEF})$). Eq. 12-21 can be used to determine the cumulative probability EEF is less than a certain value. Table 9 lists probabilities that the EEF is less than several different values.

Table 9 Probabilities Associated with the Distribution of EEF

k	$\mu_Z - k\sigma_Z$	$P(Z < \mu_Z - k\sigma_Z)$ [1]	$\exp(\mu_Z - k\sigma_Z)$	$P(EEF < \exp[\mu_Z - k\sigma_Z])$
1	0.416	2×10^{-1}	1.52	2×10^{-1}
2	0.364	2×10^{-2}	1.44	2×10^{-2}
3	0.313	1×10^{-3}	1.37	1×10^{-3}
4	0.262	3×10^{-5}	1.30	3×10^{-5}
5	0.210	3×10^{-7}	1.23	3×10^{-7}
6	0.159	1×10^{-9}	1.17	1×10^{-9}
7	0.108	1×10^{-12}	1.11	1×10^{-12}
8	0.0567	6×10^{-16}	1.06	6×10^{-16}
9	0.00543	1×10^{-19}	1.01	1×10^{-19}

[1] Probabilities were calculated using Knight (2006)